The Astrophysical Journal Supplement Series, 272:25 (22pp), 2024 June https://doi.org/10.3847/1538-4365/ad39c5

β Cephei Pulsators in Eclipsing Binaries Observed with TESS

Christian I. Eze[1,2] and Gerald Handler[1]
[1] Nicolaus Copernicus Astronomical Center of the Polish Academy of Sciences, Bartycka 18, 00-716 Warsaw, Poland; cheze@camk.edu.pl
[2] Department of Physics and Astronomy, University of Nigeria, Nsukka, Nigeria
Received 2023 October 17; revised 2024 March 14; accepted 2024 March 18; published 2024 May 14

Abstract

The combined strength of asteroseismology and empirical stellar basic parameter determinations for in-depth asteroseismic analysis of massive pulsators in eclipsing binaries shows great potential for treating the challenging and mysterious discrepancies between observations and models of stellar structure and the evolution of massive stars. This paper compiles a comprehensive list of massive pulsators in eclipsing binary systems observed with TESS. The TESS light curves and discrete Fourier transforms of a sample of 8055 stars of spectral type B0–B3 were examined for eclipses and stellar pulsations, and the ephemerides of the resulting subsample of massive pulsators in eclipsing binaries were computed. This subsample was also crossmatched with existing catalogs of massive pulsators. Until now, fewer than 30 β Cephei pulsators in eclipsing binaries have been reported in the literature. Here we announce a total of 78 pulsators of the β Cephei type in eclipsing binaries, 59 of which are new discoveries. Forty-three are recognized as definite, and 35 are candidate pulsators. Our sample of pulsating massive stars in eclipsing binaries allows for future asteroseismic modeling to better understand the internal mixing profile and to resolve the mass discrepancy in massive stars. We have already started follow-up work on some of the most interesting candidates.

Unified Astronomy Thesaurus concepts: Asteroseismology (73); Beta Cephei variable stars (148); Binary stars (154); Eclipsing binary stars (444); Massive stars (732); Multi-periodic pulsation (1078); Observational astronomy (1145); Period determination (1211); Variable stars (1761); Pulsating variable stars (1307); Space telescopes (1547); Stellar pulsations (1625)

Supporting material: machine-readable tables

1. Introduction

Asteroseismology is the study or science of determining the interior structures of stars from their oscillations/pulsations (e.g., Gough 1985; Handler 2013; Aerts 2021). These oscillations exist in the form of radial or nonradial oscillation modes. Radial oscillation modes are seen in classical pulsators (e.g., Cepheids, RR Lyr stars, and Miras) and show strong relevance in observational cosmology (e.g., Anderson & Riess 2018). On the other hand, nonradial oscillation modes are of interest in asteroseismology. They are solutions to the equations of motion of a star that gets perturbed from its equilibrium (Aerts 2021). The nonradial modes are mainly of two types, depending on which of the forces (pressure or buoyancy) is dominant in restoring the equilibrium. Modes that are restored by the pressure force are called pressure modes (*p* modes) and those that are restored by buoyancy are termed gravity modes (*g* modes). While *p* modes have large amplitudes in the envelopes of the stars and are characterized by dominant radial motions, *g* modes have large amplitudes in the deep interior of the star and are characterized by dominant horizontal motions. Mixed modes constitute another class of nonradial oscillation mode, which have a *p*-mode character in the envelope and a *g*-mode character in the deep interior and show excellent probing power in the entire star.

Massive stars also show pulsations (e.g., Bowman 2020) and offer unique opportunities to constrain their properties via asteroseismology (Aerts et al. 2010). Three classes of massive pulsators exist, namely: (1) β Cephei (β Cep) stars, which are early B-type main-sequence stars with masses of approximately 9–17 $M_{\odot}$, low radial order pressure (*p*), gravity (*g*), and mixed modes, pulsation amplitudes up to a few tenths of a magnitude, and pulsation periods of several hours (approximately 2–6 hr; e.g., Sterken & Jerzykiewicz 1993; Aerts & De Cat 2003; Stankov & Handler 2005; Handler 2013); (2) slowly pulsating B (SPB) stars, which are mid-to-late B stars of masses 3–9 $M_{\odot}$ with high radial order *g* modes and observationally challenging periods of the order of days (approximately 0.5–4 days; e.g., Waelkens 1991; Waelkens et al. 1998); and (3) a group that shows stochastic low-frequency (SLF) variability and has quasiperiodic and time-dependent variability spanning a broad range of periods from the order of minutes to several days (e.g., Bowman et al. 2019a, 2019b, 2020). Following the relative abundance of pulsators of spectral type B compared to O stars, the majority of the constraints on the stellar structure and evolutionary theory of massive stars are currently believed to come from β Cep and SPB stars (Aerts et al. 2019; Bowman et al. 2020). β Cep stars are adjudged to be supernova progenitors and their roles in shaping galaxy dynamics or its chemical enrichment are crucial. Although they predominantly pulsate in *p* modes (Stankov & Handler 2005), they also have *g* and mixed pulsation modes (e.g., Handler et al. 2017). These make them very important in seismically probing the entire star. Their understanding gives us insight into the properties of massive stars, such as rotational mixing, convective core overshooting, etc., as well as the transition from main sequence to hydrogen-shell burning evolution of massive stars (Neilson & Ignace 2015). Owing to these features, especially core convection, the uncertainties in the stellar structure and evolution theory are largest for stars of the O and B categories (Pedersen et al. 2019) and hence compound the problem or mystery of mass discrepancy in massive stars. The mass discrepancy problem involves situations where the masses of stars inferred from spectroscopy are different from the masses derived from models of stellar evolution (Herrero et al. 1992; Tkachenko et al. 2020).

Massive stars are predominantly found in multiple systems (Sana et al. 2012, 2014; Kobulnicky et al. 2014; Southworth & Bowman 2022a), hence a substantial fraction are expected to also be located in eclipsing binaries. Southworth (2012), in line with Russell (1948) and Batten (2005), described eclipses as the royal road to stellar astrophysics. By modeling eclipses, model-independent precise stellar parameters (e.g., radius and mass), which serve as invaluable calibrators for stellar evolution theory (Torres et al. 2010; Pedersen et al. 2019), are obtained. Dynamical masses deduced from eclipsing binary modeling and asteroseismic masses offer unique opportunities to constrain the physics of stellar evolution models to treat the challenging and mysterious discrepancies between observations and models (Tkachenko et al. 2020). Unfortunately, the absolute numbers of reported massive stars in eclipsing binary or multiple systems are significantly smaller compared to their low-mass counterparts (Kirk et al. 2016; Pedersen et al. 2019). However, TESS (Ricker et al. 2015) is out to change this narrative. It is the first precision photometry mission that surveys (almost) the whole sky and it has released, in large amounts, time-resolved photometry of stars of O and B spectral types (e.g., Handler et al. 2019) with a precision comparable to Kepler and K2, but for stars five magnitudes brighter, owing to its smaller telescope aperture. Since the advent of the TESS mission, there has been a concerted effort by researchers in the field to obtain a comprehensive and adequate sample size of massive pulsators for massive star asteroseismology, to improve the physics of the stellar structure and evolution models of massive stars using TESS data. These efforts are to compensate for the lack of a sufficient number of such stars observed with high-precision space photometry prior to TESS (Aerts et al. 2010; Handler 2013) and to gather a pool of suitable candidates for in-depth asteroseismic analysis. This major barrier of the small sample size has thus far hampered the general asteroseismic understanding of high-mass stars.

A number of authors have published catalogs of massive stars in the recent past. Pedersen et al. (2019) presented a classification of the variability of 154 massive stars with spectral types O and B that were observed by TESS at short cadence (2 minutes). Their sample consisted of single or binary stars of diverse variability and was aimed at establishing an unbiased sample for O and B stars for future asteroseismology. A similar search was conducted by Burssens et al. (2020), who combined the TESS photometry with spectroscopy, allowing the stars to be more accurately placed on the H-R diagram. Forward asteroseismic modeling of single β Cep stars has also been conducted by Burssens et al. (2023).

To combine the strengths of eclipsing binary modeling and asteroseismology, a lot of other recent searches have been either narrowed down to massive pulsators in eclipsing binary systems or done on larger scales to capture more massive eclipsing binaries in the sample (Southworth 2015; Southworth et al. 2020, 2021; IJspeert et al. 2021; Zari et al. 2021; Southworth & Bowman 2022a). While some of these authors focused mainly on identifying eclipsing binaries, these works still play a significant role in the search for β Cep pulsators in eclipsing binaries, as they provide lists of already existing eclipsing binaries. Whereas Southworth (2015), Southworth et al. (2020, 2021), and Southworth & Bowman (2022a) have small numbers of massive pulsators in their samples, as they considered a heterogeneous sample of pulsating eclipsing binaries with predominantly short orbital periods (<27 days), owing to having 1+ TESS sectors, IJspeert et al. (2021), on the other hand, published a large sample of massive stars comprising single stars and eclipsing binaries in their effort to identify eclipsing binaries in OBA-type stars. However, they limited their search to stars of TESS magnitude below 15 with color indices $J - H < 0.045$ and $J - K < 0.06$. There is a large overlap between the catalog of OBA-type stars compiled by IJspeert et al. (2021) and that compiled by Zari et al. (2021), which used a Gaia magnitude cut of $G < 16$ as one of their major selection criteria. Here, we aim to compile a comprehensive catalog of early B-type (B0–B3) pulsators in eclipsing binaries observed by TESS, with a particular focus on β Cep stars, in order to harness the combined potentials of eclipsing binary stars and asteroseismology to probe the evolution and properties of massive stars. The spectral range we selected is expected to yield a comprehensive homogeneous sample of massive main-sequence pulsators with the self-excited *p, g*, and mixed modes needed for the overall asteroseismic probe of massive pulsators. In Section 2, we describe the sample, its observation and selection criteria. In Section 3, we describe the analysis. We discuss the results of the variability classification and periodicity of the pulsators in our sample in Section 4, and we draw the necessary conclusions in Section 5.

2. Sample Selection and Observation

The primary photometric data used for this work are the TESS 30 minutes cadence light curves (Quick-Look Pipeline (QLP) data; Huang et al. 2020a, 2020b) obtained from the Barbara A. Mikulski Archive for Space Telescopes (MAST) and observed in the first two cycles of TESS, covering sectors 1–26. The QLP light curves of 8055 stars of spectral type B0–B3 were analyzed. The list of the stars was first obtained from a compilation of published spectral type catalogs done by Balona (2022) and the TESS light curves downloaded from MAST. For stars in our sample with available 2 minutes cadence data at the time of this work, we also examined the 2 minutes cadence light curves. The sample spans ranges of 3.23–12.33 in V magnitude and 3.01–12.96 in B magnitude, respectively. As a result, it includes both bright and faint stars with varying morphology. In terms of morphology, eclipsing binary stars are classified as detached, semidetached, and overcontact binaries (see Kallrath & Milone 2009 for details). While detached eclipsing binaries are more convenient to work with, by comparing an ensemble of detached binaries with those experiencing strong tidal forces, one understands the importance and role of tidal forces in the internal processes (IJspeert et al. 2021). Hence, our search is not restricted to detached eclipsing binaries but also includes massive β Cep pulsators in eclipsing binaries of different *morphological classifications* with self-excited pulsations. Irrespective of the importance of SLF variables in the study of massive stars via internal gravity waves, we ignored them during the selection of pulsators from our sample. We also ignored the SPBs in our sample during the selection, owing to their mass range, which is not within the β Cep regime of interest. However, any hybrid

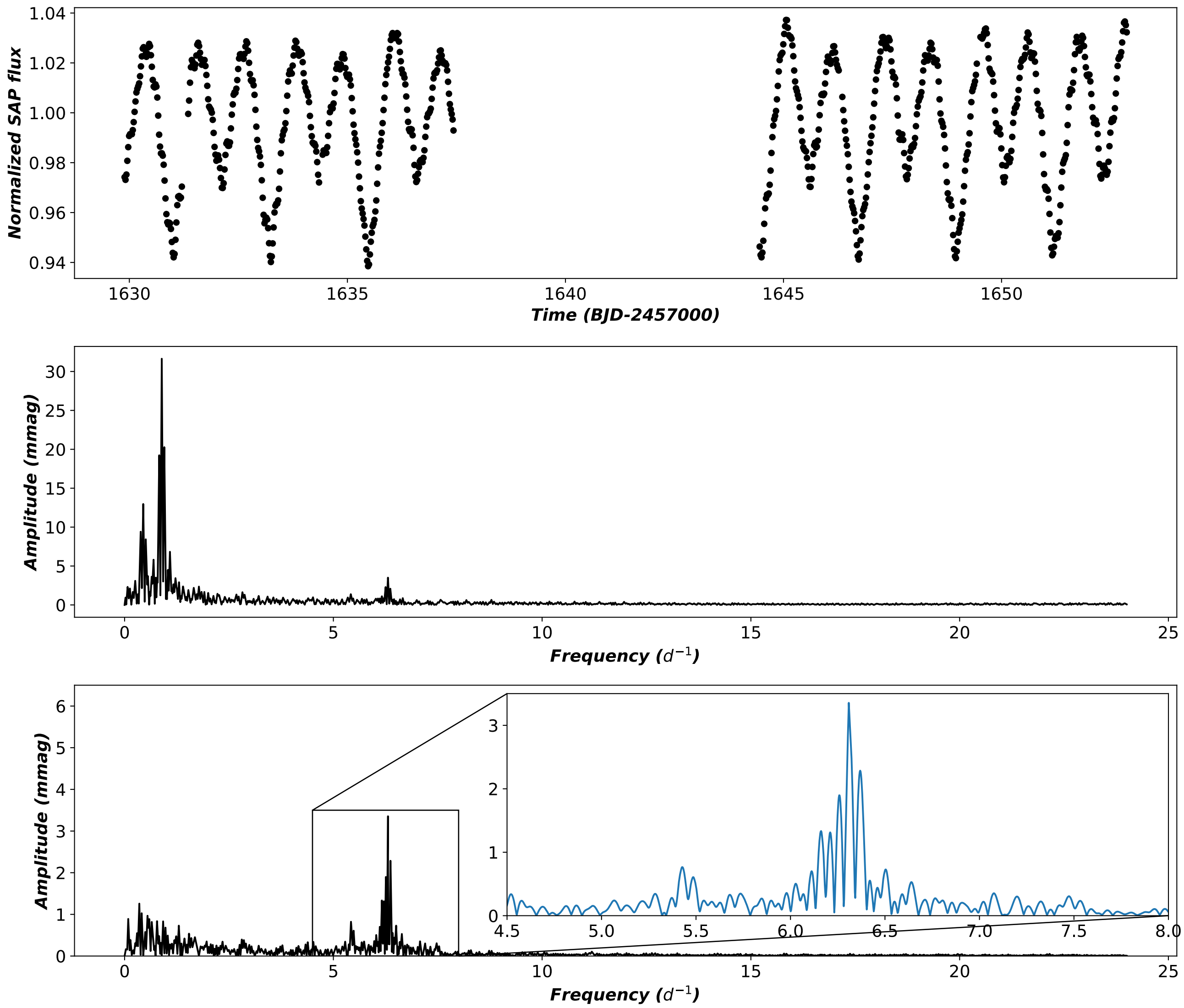

Figure 1. An example figure of the light curve and DFT of a massive pulsator in eclipsing binaries (HD 329379) in our sample. The upper panel shows the TESS light curve. The middle panel shows the DFT of the light curve shown in the upper panel, whereas the lower panel shows the DFT of the residual light curve after removing the orbital light variations. The region showing the dominant β Cep pulsations is also zoomed in on and shown in the inset in the lower panel.

massive pulsator with self-excited pulsations and a β Cep component was included in the sample of pulsators. Hereinafter, we shall refer to the entire list of the stars examined as "the sample" and refer to the list of eclipsing binaries in the sample with a β Cep pulsating component(s) as "the sample of pulsators."

3. Analysis

To preselect candidates, we first plotted the light curves and the discrete Fourier transforms (DFTs) of each of the 8055 stars. Via visual examination of the plots, stars that show eclipses as well as frequency peaks in the regimes of β Cep were preselected. Here, we considered pulsations with frequencies $f \geqslant 3\,\mathrm{day}^{-1}$ as β Cep pulsations. Owing to the effect of binarity, some of the frequency peaks adjudged to be independent frequencies sometimes appear to be harmonics of the orbital frequency or could be hidden within a forest of peaks in the DFT caused by the orbital light variations. In a few cases, the pulsational signals were of higher amplitude than the eclipses, which would then manifest themselves as a series of low-frequency harmonics in the DFT. As a result, successive prewhitening of each of the light curves of the stars in the preselected sample was done using the *Period04* software (Lenz & Breger 2005).

The *Period04* software (Lenz & Breger 2005) applies discrete-frequency Fourier analysis and simultaneous multi-frequency least-squares fitting. Calculations of light-curve fits for multiperiodic signals such as harmonics, combination, and equally spaced frequencies are also possible in the program. To remove the effect of binarity from the light curve, we fitted the orbital frequency and all its detected harmonics and subtracted the fit from the light curve, resulting in a residual that would contain the pulsational signals only. We further prewhitened this residual to check for independent frequency peaks. For the prewhitening, we used an upper frequency of $23.5\,\mathrm{day}^{-1}$, which is slightly below the Nyquist frequency, and accepted independent pulsation frequencies with a signal-to-noise ratio $(\mathrm{S/N}) \geqslant 4.6$ as real frequencies (see Baran & Koen 2021). For the sake of this classification, we did not do exhaustive prewhitening of the residual to extract all the frequencies. Since our interest is to compile massive pulsators and not the exact

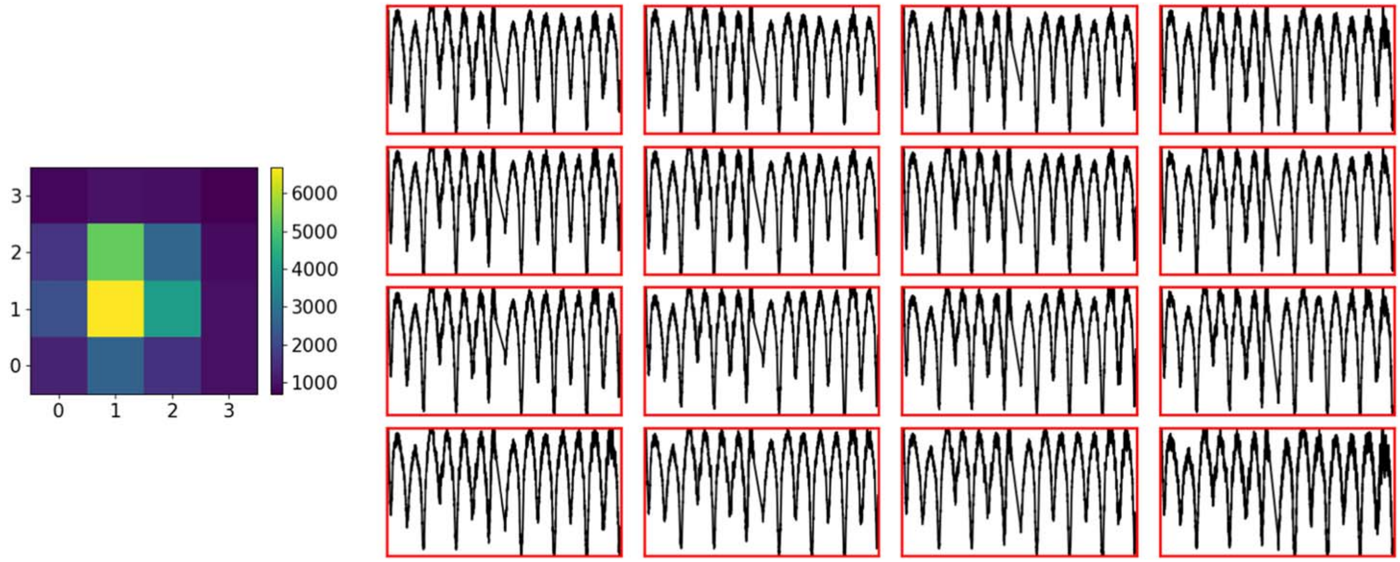

Figure 2. A cutout session of the pixel-to-pixel plot of the aperture mask for V1216 Sco.

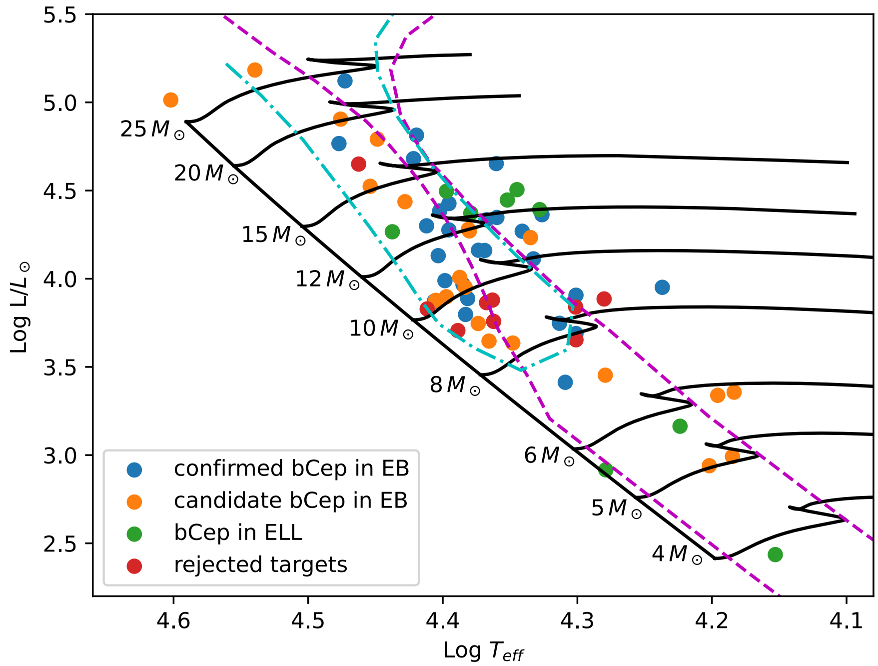

Figure 3. H-R diagram of the stars listed in Tables 1–4. The dashed magenta line denotes the SPB instability strip, whereas the dashed–dotted cyan line denotes the β Cep instability strip. Stars with missing parameters (e.g., A_0, $T_{\rm eff}$) are not captured in the H-R diagram.

number of pulsations they have, we only considered at least one to five dominant peaks, and in cases where hybrid pulsation is suspected, we continued the prewhitening until the given object could be established or disproved as a hybrid pulsator. For frequencies between 2 and 4 day^{-1}, it is difficult to classify the pulsators as β Cep, SPB, or hybrid using only the frequency range, owing to the fact that rotation can split multiplets of nonradial p and g modes into the regimes of each other. Combination frequencies can also fall into this frequency domain. The latter have been checked for and are not used to classify the variability. A small number of stars do show signals between 2 and 4 day^{-1}, but determining their exact cause is outside the scope of this work. Figure 1 shows an example light curve and DFT of a hybrid pulsator in the sample.

The stars in the preselected sample that have shown independent pulsation peaks were subjected to further checks for false eclipses and blends. The light curves of the stars (especially in crowded regions on the sky) are sometimes modulated by stray light from neighboring stars that blends with their light. Owing to blends, there have been incidences of false eclipses in stars or pulsations wrongly attributed to stars that they do not originally come from. To correct for blends, we conducted photometric checks and analyses using Eleanor v2.0.5 (Feinstein et al. 2019). Eleanor is an open-source Python-based package used for the downloading, extraction, analysis, and visualization of flux-corrected light curves from TESS Full Frame Images (FFIs). It is also used for the crossmatching of light curves. It takes, as input, a TESS input catalog ID, coordinates (R.A., decl.), or a Gaia source ID of a

Table 1
List of Definite β Cep Pulsators in Eclipsing Binary Systems with Their Orbital Ephemerides and Dominant Pulsation Frequencies

Name	TIC ID	R.A.	Decl.	Variability	*B*mag	*V*mag	*P* (day)	*T* (BTJD)	*F* (day^{-1})	*A* (mmag)	S/N	SpType	References
16 Lac	129538133	22 56 23.63	+41 36 13.95	EB+bCep	5.44	5.59	12.0951(5)	1748.220(2)	5.9112(2)	6.19(6)	127.9	B2IV	L10, J80, W51
λ Sco	465088681	17 33 36.52	−37 06 13.76	EB+bCep	1.49	1.63	5.949(1)	1635.023(30)	4.68035(7)	6.64(2)	49.6	B2IV+DA7.9	SWB22a
BD+44 3594	353099086	20 49 11.59	+45 24 39.79	EB+bCep+SPB	10.37	9.85	>33	2809.36(40)	6.8169(9)	0.75(7)	16.6	B1:V:nep	⋯
BD+44 3664	330081196	20 59 55.99	+45 20 12.94	EB+bCep	10.64	10.15	4.80323(6)	1713.45(5)	7.4862(1)	7.03(4)	66.8	B1Vn/B9	⋯
CD−38 4128	134522557	08 09 28.64	−38 51 29.28	EB+bCep	10.12	9.75	5.730(2)	1494.955(22)	5.67991(6)	6.47(2)	93.7	B1V	BO20
CD−51 9984	314529804	16 18 22.91	−51 26 24.27	EB+bCep	10.59	10.25	9.79258(3)	1632(6)	5.744(2)	5.9(4)	11.6	B0.5III	BO20
CPD−41 7746	339570153	16 54 29.49	−41 39 14.95	EB+bCep	9.47	9.24	6.3467(3)	1633.57(10)	8.3307(2)	1.87(2)	56.8	B0.5V	⋯
CPD−45 3109	28957011	08 49 35.49	−46 23 19.27	EB+bCep	9.79	9.58	2.7139(1)	1519.1(2)	5.18739(7)	11.76(8)	56.4	B2/4	⋯
CZ Vel	355656323	09 10 44.46	−50 42 40.61	EB+bCep	11.57	10.80	5.1929(1)	1519.35(20)	4.5871(5)	2.9(1)	33.4	B2III/B6	DK04
EK Cru	379012185	12 02 58.47	−62 40 19.23	EB+bCep+ SPB	8.10	8.11	4.7447(1)	1572.36(10)	6.1436(2)	0.54(1)	41.2	B1V	OW05
EO Aur	408937625	05 18 21.07	+36 37 55.36	EB+bCep	7.90	7.83	4.06550(3)	1830.47762(5)	12.1462(5)	0.75(1)	40.7	B0V+B3V	SWB22a
HD 108628	450918869	12 29 06.03	−62 28 00.15	EB+bCep	10.04	9.76	4.222(5)	1600.47(7)	6.7419(5)	2.34(5)	46.9	B2II	PP08
HD 112026	436382800	12 54 18.43	−60 53 38.93	EB+bCep	8.69	8.66	43.205(1)	1622.06(20)	6.3869(4)	2.22(4)	46.9	B0/1IV	⋯
HD 112485	437617380	12 57 51.50	−60 48 56.08	EB+bCep	9.57	9.53	5.372(1)	1604.95(90)	9.439(1)	1.16(6)	20.3	B1/3(III)	IJ21
HD 113742	440817830	13 06 53.75	−61 56 38.01	EB+bCep	9.53	9.20	15.68844(8)	1600.43(10)	6.936(1)	0.66(4)	10.1	B1/2(III)	⋯
HD 150927	78636551	16 45 44.06	−38 10 02.80	EB+bCep	9.68	9.42	14.33(2)	1629.95(20)	4.84325(2)	116.99(9)	186	B2/3Ib	PP08
HD 151791	246552414	16 51 35.18	−44 29 35.79	EB+bCep	9.73	9.50	3.9173(1)	1631.97(20)	5.227(1)	0.68(4)	25.2	B2/3Ib/II	⋯
HD 152268	339680203	16 54 16.59	−40 58 59.25	EB+bCep	8.97	8.98	3.4229(5)	1630.75(10)	10.0996(8)	1.19(4)	35.9	B1/2Ib/II	IJ21
HD 157400	158688754	17 24 36.89	−35 50 19.75	EB+bCep	10.10	9.68	8.4527(4)	1630.5(2)	11.8628(7)	1.22(4)	20.3	B3/5	⋯
HD 188891	171502734	19 55 44.76	+40 23 30.25	EB+bCep+SPB	7.29	7.30	161.25	1731.0(4)	4.971(1)	0.67(8)	5.3	B1V	IJ21
HD 227877	91111448	20 08 23.07	+35 27 33.48	EB+bCep	9.37	9.3	1.70664(4)	1683.68(5)	13.2182(5)	0.88(4)	36.2	B1:IV:nn	C22
HD 254346	426520557	06 16 57.32	+22 11 41.96	EB+bCep	10.13	9.74	5.4316(1)	2478.5(2)	9.2399(2)	0.256(6)	23.6	B2:III:	LB20
HD 303115	458263480	10 38 33.37	−59 21 31.65	EB+bCep	10.57	10.30	4.618(1)	2286.35(50)	5.73966(4)	8.65(3)	181.9	OB-/B5	⋯
HD 329379	122314621	17 01 05.87	−45 42 04.24	EB+bCep+SPB+ELL	10.70	9.83	2.2464(4)	1631.0(3)	6.3086(8)	3.4(1)	53.3	B0II	⋯
HD 339003	10891640	19 51 02.86	+25 57 15.43	EB+bCep	10.43	9.93	6.163(2)	1685.1(2)	6.7993(3)	12.6(2)	43.1	B0.5III	LB20
HD 344880	451932686	19 45 42.31	+23 59 04.03	EB+bCep	9.96	9.34	54.49399(1)	1683.6(4)	9.4923(8)	1.83(7)	32.9	B0.5III:nn	LB20
HD 92024	458076434	10 36 08.33	−58 13 04.36	EB+bCep	8.90	9.00	8.3249(8)	2285.135(40)	7.1635(1)	5.59(3)	41.4	B1III	F05
HD 96355	466528132	11 05 26.38	−61 26 04.20	EB+bCep	9.87	9.74	4.360(2)	1574.336(20)	6.350(2)	0.26(2)	16.7	B0/1(III)	IJ21
HQ CMa	106830354	07 20 54.92	−26 57 49.81	EB+bCep/SPB	5.82	5.99	⋯	⋯	⋯	⋯	⋯	B3V	SWB22a
LR Ara	447530589	16 53 37.19	−61 35 11.27	SPB?+bCep+EB	10.60	10.70	1.5195(3)	1626.92(22)	4.498(2)	0.62(6)	7.5	B2	BD80
LS I+61 145	406965391	00 22 26.52	+61 49 39.75	EB+bCep	11.30	10.90	1.84633(5)	1767.71(10)	7.540(2)	0.29(2)	9.9	B1V	IJ21
LS I+63 36	359042331	00 05 00.85	+63 49 33.21	EB+BCep+DSCT?	11.52	11.06	⋯	1782(12)	4.319(1)	1.1(1)	10	B0V	⋯
TYC 3699-160-1	245470639	02 35 50.71	+58 35 20.83	EB+bCep+SPB	13.00	12.33	3.0687(9)	1794.42(10)	5.819(1)	2.0(1)	20.8	B0	⋯
TYC 4050-2830-1	458879750	02 22 45.39	+62 25 36.98	EB+bCep+SPB	11.77	11.53	11.039(6)	1799.506(9)	9.239(1)	0.57(3)	13.4	B3	⋯
V1061 Cen	334443373	14 14 56.81	−61 14 18.42	EB+bCep	9.71	9.56	2.2096(3)	1600.68(10)	10.142(6)	0.22(6)	9.3	B2II/III	OT03
V1166 Cen	443262289	13 15 51.32	−63 53 03.32	EB+bCep	8.84	8.81	13.4551(3)	1604.35(20)	10.155(1)	1.17(6)	24.2	B1/2V	AG12
V1216 Sco	247315421	16 54 57.71	−43 56 27.17	EB+bCep	10.93	10.17	3.9213(6)	1632.95(15)	5.5517(5)	10.6(2)	38.2	B0	OT03
V2107 Cyg	42244951	20 08 45.77	+37 14 13.36	EB+bCep/SPB	8.73	8.63	4.2846(4)	1712.70759(6)	4.2008(3)	3.43(9)	25.3	B1III	SWB22a
V4386 sgr	60433558	18 14 42.14	−33 08 27.22	EB+bCep	8.30	8.44	10.798(1)	1664.20(20)	6.7726(3)	7.63(9)	78.8	B1II	PP08, C22
V453 Cyg	90349611	20 06 34.97	+35 44 26.27	EB+bCep	8.52	8.40	3.8900(4)	1684.2(1)	4.9459(2)	3.05(4)	47.7	B0.4IV+B0.7IV	SW20
V916 Cen	322078735	11 42 25.35	-62 28 37.47	EB+bCep	9.68	9.63	1.46322(5)	1573.1113(60)	4.451427(6)	13.2(1)	66.7	B0.5IVne	PP08
VV Ori	50897998	05 33 31.45	−01 09 21.86	EB+bCep+SPB	5.16	5.34	1.4853(2)	1468.45(10)	9.179(3)	1.5(2)	18.9	B1V+B4.5V	SW21
VZ Cen	304803692	11 52 28.76	−61 31 26.93	EB+bCep	8.36	8.36	4.92870(2)	1574.95(20)	6.03025(7)	3.88(3)	67.1	B2III/IV	IJ21

Note. *P* is the period, *T* is the epoch given in BTJD, *F* is the dominant β Cep pulsation, *A* is the amplitude of the dominant β Cep pulsation, and SpType is the spectral type of the star. The dominant β Cep pulsations and their amplitudes are given with their analytical errors.

References. L10: Lee (1910); J80: Jerzykiewicz (1980); W51: Walker (1951); SWB2a: Southworth & Bowman (2022a); BO20: Balona & Ozuyar (2020); DK04: Dvorak (2004); OW05: Otero & Wils (2005); PP08: Pigulski & Pojmański (2008); IJ21: IJspeert et al. (2021); C22: Chen et al. (2022); LB20: Labadie-Bartz et al. (2020); F05: Freyhammer et al. (2005); BD80: Brancewicz & Dworak (1980); OT03: Otero (2003); AG12: Alfonso-Garzón et al. (2012); SW20: Southworth et al. (2020); and SW21: Southworth et al. (2021). SA00, BM22, DR10, SWB22b, and K68 in Table 2 refer to Shibahashi & Aerts (2000); Drobek et al. (2010); Southworth & Bowman (2022b); Bowman et al. (2022); and Kukarkin et al. (1968), respectively. These authors classified the stars as eclipsing binaries or β Cep pulsators or both. The details of their classifications and other brief information about the stars are given in the Appendix.

(This table is available in machine-readable form.)

Table 2
List of Candidates for β Cep Pulsators in Eclipsing Binaries with Their Orbital Ephemerides and Dominant Pulsation Frequencies

Name	TIC ID	R.A.	Decl.	Variability	*B*mag	*V*mag	*P* (day)	*T* (BTJD)	*F* (day^{-1})	*A* (mmag)	S/N	SpType	References
23 Ori	264592553	05 22 50.00	+03 32 40.05	EB+bCep?	4.86	5.00	4.56(1)	1470.805(20)	11.7727(8)	1.90(6)	43.9	B2IV/V	IJ21
β Cep	321818578	21 28 39.59	+70 33 38.57	EB+bCep?	3.01	3.23	4.6083(9)	2856.233(50)	5.249626(4)	13.739(9)	37.3	B0.5IIIs	SA00, BM22
AN Dor	220430912	04 52 28.24	−55 41 49.41	EB+bCep/SPB?	7.47	7.69	2.032671(3)	2155.71301(1)	3.20275(4)	1.21(3)	27.4	B2/3V	SWB22a
CD−28 5247	130348163	07 59 44.31	−29 00 55.16	EB+bCep?	11.75	11.33	4.256(2)	1495.362(20)	4.976(2)	0.53(5)	8.9	B0V/Obe	
CD−32 4839	144535458	08 05 56.85	−33 00 21.91	EB+bCep?	12.21	11.57	4.1317(5)	2229.6(6)	5.097(1)	1.0(1)	9.8	B2/4	
CD−32 4971	145760541	08 12 21.08	−32 35 03.34	EB+bCep?	11.00	10.70	8.787(2)	2232.5(3)	5.3263(6)	1.69(9)	19.6	B1IV	
CD−44 4813	28699677	08 46 53.39	−44 43 20.06	EB+bCep?	11.29	10.74	22.9444(5)	1548.92(30)	4.4475(7)	0.29(2)	7.7	B2/5	
CD−57 3146	463899225	10 19 12.87	−58 26 01.03	EB+bCep?	10.77	10.73	23.283(8)	1564.925(23)	5.0817(3)	1.84(5)	28.9	B3/4	IJ21
GSC 04052-01378	390515222	02 53 08.35	+62 06 10.49	EB+bCep?	⋯	11.70	18.310(6)	1798.018(10)	3.0631(2)	5.03(8)	36.1	B2	⋯
HD 101838	321947833	11 42 49.28	−62 33 54.98	EB+bCep?	9.56	9.55	5.41187(7)	1574.645(10)	3.12772(3)	10.72(3)	19.52	B0.5/1III	PP08, DR10
HD 135477	455667423	15 18 06.61	−60 05 38.91	EB +bCep+SPB?	8.15	8.20	2.0079(3)	1626.205(60)	5.895(3)	0.22(4)	5.9	B2V	IJ21
HD 138112	284374921	15 32 54.50	−59 48 26.29	EB+bCep?	9.63	9.51	21.037(6)	2345.70(20)	5.153(1)	0.23(3)	4.97	B2IV-V/B5	IJ21
HD 13969	264613302	02 17 49.85	+57 05 25.58	EB+bCep?	9.15	8.02	16.305(5)	2887.34(50)	7.1265(6)	0.62(2)	19	B0.5I	⋯
HD 143605	427406031	16 04 15.99	−56 26 27.39	EB+bCep?	9.23	9.15	2.2077(2)	1627.96(2)	4.963(4)	0.20(4)	5.2	B3V	⋯
HD 151083	51288359	16 47 51.39	−51 46 04.05	EB+bCep?	10.08	9.54	1.8016(4)	1632.945(50)	6.242(2)	1.9(2)	16.2	B2Vn	⋯
HD 154407	42424196	17 06 47.90	−35 53 15.07	EB+bCep?	9.12	8.83	2.5592(4)	1631.54(10)	12.968(2)	0.35(4)	10.6	B2Vn	⋯
HD 155274	45731009	17 11 57.77	−35 00 26.32	EB +bCep+SPB?	10.14	9.73	6.896(7)	1629.9744(50)	10.143(1)	1.15(5)	37.6	B2/5(n)	⋯
HD 1743	428415975	00 22 03.41	+62 11 06.29	EB+bCep?	8.43	8.33	11.7950(5)	1801.35(36)	8.7933(6)	0.24(6)	12.9	B0.2IV	IJ21
HD 240171	314034024	23 02 44.51	+57 08 33.51	EB+bCep?	10.02	9.92	5.1514(9)	1630.75(10)	7.65284(7)	1.29(4)	37.8	B1V	⋯
HD 277680	122883754	05 10 17.68	+40 39 35.26	EB+bCep?	8.93	8.89	4.3207(5)	1818.8(2)	8.4876(9)	0.95(4)	28	B3	IJ21
HD 306124	466887289	11 08 51.19	−61 21 10.48	EB+bCep?	10.89	10.68	1.4074(8)	2310(4)	5.545(5)	0.12(3)	4.9	B3	⋯
HD 46060	25041731	06 30 49.81	−09 39 14.80	EB+bCep?	9.03	8.82	20.6094(8)	1474.22(20)	9.9603(9)	0.38(1)	25.6	B2II	⋯
HD 73903	141497319	08 38 58.88	−46 13 37.55	EB+bCep?	9.19	9.05	2.8093(2)	1520.19(20)	4.25210(7)	15.19(9)	94.9	B3II	⋯

Table 2
(Continued)

Name	TIC ID	R.A.	Decl.	Variability	*B*mag	*V*mag	*P* (day)	*T* (BTJD)	*F* (day^{-1})	*A* (mmag)	S/N	SpType	References
HD 76838	30562668	08 57 07.55	−43 15 22.27	EB+bCep?	7.31	7.31	3.8522(2)	1518.08(40)	8.7329(1)	2.84(3)	93.9	B2IV	C22
HD 92741	458561474	10 41 12.35	−59 58 25.04	EB+bCep?	7.22	7.25	5.373(2)	1574.57(20)	4.9674(1)	2.72(4)	47.7	B1/2II	IJ21
HD 92782	458599043	10 41 30.95	−57 30 51.61	EB+bCep?	9.62	9.51	14.46(2)	2287.375(20)	6.52581(6)	12.02(3)	65.9	B1/2(III)	···
Hilt 1208	269228628	23 17 13.69	+60 00 27.93	EB+bCep?	11.35	10.90	2.422(1)	2856.38(4.00)	4.99209(4)	8.04(3)	120.4	B2	LB20
LS VI -04 19	33091633	06 59 30.23	−04 48 43.82	EB+bCep?	11.10	10.81	7.520(4)	1495.83(30)	10.564(1)	0.51(2)	20.5	B0IV	···
NGC 2483 2	129364361	07 55 43.58	−27 54 05.42	EB +bCep+SPB?	12.46	12.16	4.767(5)	1493(3)	4.162(1)	1.9(2)	11.56	B3	
QX Car	469247903	09 54 33.88	−58 25 16.58	EB+bCep?	6.47	6.64	4.47800(2)	1546.32(10)	5.722(2)	0.13(2)	5.5	B2V	SWB22a
TYC 8995-5052-1	314139276	13 30 00.85	−63 38 04.24	EB+bCep?	11.77	11.43	4.73(1)	1665.5301(40)	5.896(3)	12.4(1.7)	16.9	B2III	···
V1388 Ori	337165095	06 10 59.17	+11 59 41.48	EB +bCep+SPB?	7.44	7.50	2.1870301(8)	2485.226609(16)	3.9987(8)	0.18(5)	5	B2V	SWB22b
V446 Cep	335265326	22 08 45.59	+61 01 20.71	EB+bCep?	7.40	7.32	3.808386(6)	1767.0005(1)	10.24378(1)	1.280(7)	93.5	B1V	IJ21,SWB22a
V536 Mon	23548300	07 13 55.57	−02 54 29.87	EB +bCep+SPB?	9.29	9.41	6.1341(3)	1493.21(20)	6.541(2)	0.44(3)	20.5	B3/4III	K68
V964 Sco	339567760	16 54 18.32	−41 51 35.65	EB+bCep?	9.78	9.60	5.2179(5)	2366.63(20)	11.3812(3)	1.70(3)	23.4	B0.5V	···

Note. The dominant β Cep pulsations and their amplitudes are given with their analytical errors.

(This table is available in machine-readable form.)

Table 3
List of Ellipsoidal Variables with β Cep Pulsating Components

Name	TIC ID	R.A.	Decl.	Variability	*B*mag	*V*mag	*P* (day)	*F* (day^{-1})	*A* (mmag)	S/N	SpType	References
BD+48 658	301263808	02 23 23.60	+49 01 55.41	EB/ELL+BCep	8.65	8.76	2.955(2)	6.1044(8)	1.74(6)	37.7	B2	⋯
HD 13338	347486043	02 12 19.17	+57 56 27.17	ELL/ROT+bCep	9.38	9.17	⋯	4.63533(9)	5.548(9)	11.8	O9.5V/B1III	LB20
HD 232874	266338052	04 02 15.74	+53 45 11.78	EB/ELL+bCep	9.26	8.92	1.5174(8)	5.7395(3)	7.59(9)	11.2	B0.5V	LB20
HD 277132	121064859	04 56 27.87	+41 16 18.94	EB/ELL/ROT+bCep	11.58	11.23	2.4291(4)	4.621(4)	0.7(1)	9.3	B3	⋯
HD 300978	458604640	10 41 55.77	−56 42 51.88	EB/ELL/ROT+bCep	9.66	9.61	4.787(8)	7.6876(1)	1.69(2)	31.2	B3	⋯
HD 308106	465870314	10 58 11.89	−62 09 36.41	ROT/ELL/EB+bCep	10.77	10.65	1.8837(6)	13.709(1)	0.36(5)	6.6	B3	⋯
HD 327010	382486122	17 11 42.98	−42 52 02.75	bCep+ELL?	10.36	9.80	7.5537(6)	4.7824(9)	2.48(9)	27.8	B3	⋯
HD 39716	66975228	05 54 03.33	−06 45 08.27	ELL?+SPB?+bCep?	8.50	8.52	2.4903(3)	5.4376(9)	0.39(2)	24.9	B3III	⋯
HD 55687	178374964	07 13 34.03	−10 29 25.34	EB/ELL+SPB?+bCep	9.27	9.34	1.211(1)	7.82(1)	0.4(5)	7.6	B3II/III	⋯
NGC 6913 82	14621767	20 24 50.37	+38 18 34.60	EB/ELL+bCep	12.96	11.53	2.0499(1)	6.9686(2)	2.46(4)	34.9	B2IV	⋯

Note. The dominant β Cep pulsations and their amplitudes are given with their analytical errors.

(This table is available in machine-readable form.)

Table 4
List of Rejected Targets

Name	TIC ID	R.A.	Decl.	*B*mag	*V*mag	*P* (day)	SpType
η Ori	4254645	05 24 28.62	−02 23 49.73	3.18	3.35	7.989(3)	B1V+B2
BD+61 675	84342607	04 07 44.08	+62 18 04.13	10.16	9.61	2.699(7)	B1Vn
CD−59 4169	383089500	12 14 33.31	−60 24 40.92	11.15	10.72	2.97154(9)	B1V
CPD−59 3141	467066902	11 11 14.84	−60 29 51.08	11.25	11.06	11.5089(4)	B2
CW Cep	434893323	23 04 02.23	+63 23 48.72	7.97	7.60	2.72914(3)	B1.5Vn
FZ CMa	125497512	07 02 42.61	−11 27 11.57	8.28	8.14	1.2733(3)	B2IVn
HD 153772	212415990	17 04 01.23	−51 05 01.15	8.38	8.32	⋯	B2V
HD 154646	380870688	17 09 01.58	−46 16 38.61	9.96	9.64	13.0298(1)	B2II
HD 217919	434723918	23 03 01.47	+63 41 53.35	8.75	8.20	16.2080(9)	B3
HD 308111	465869053	10 57 54.75	−62 17 35.73	10.62	10.59	2.4396(5)	B2
LS II +23 34	360661624	19 44 21.08	+23 17 05.90	12.30	11.82	10.2572(2)	B
LS CMa	63427664	07 01 05.95	−25 12 56.28	5.47	5.64	>10	B2/3III/IV
V Pup	269562415	07 58 14.44	−49 14 41.68	4.24	4.41	1.45453(3)	B1Vp+B2

(This table is available in machine-readable form.)

star observed with TESS and returns, as a single object, a light curve and accompanying target pixel data. It allows one to plot and visualize pixel-to-pixel light curves and periodograms and possibly match the flux-corrected light curves with the existing TESS light curves or overlay the target with the Gaia sources in the field. Eleanor also uses TESS-Point (Burke et al. 2020), which is a high-precision TESS pointing tool that converts coordinates given in R.A. and decl. to the TESS detector pixel coordinates, and TESScut (Brasseur et al. 2019), which is a tool that makes a cutout, for a given region of the sky, of a TESS FFI time series, under the hood to extract its data products. Using Eleanor, we extracted the TESS target pixel files and plotted color-coded pixel-to-pixel flux-corrected light curves and DFTs of the target(s) where blends are suspected. For targets where the Eleanor default aperture appeared not to be very suitable, we defined a custom aperture mask by visually examining the pixel data and defining an optimal aperture size that captures most of the light from the target, without reducing the size to an extent that could compromise the quality of the light curves that would be extracted. Figure 2 shows the cutout session of the aperture and pixel-to-pixel light curves of one of our targets (V1216 Sco). Whereas the Eleanor light curves could be used independently for our further detailed analysis, we used them only as a photometric checking tool, for targets that could be blended, to ascertain whether or not the signatures of eclipses and pulsations observed in the QLP light curves were also present in the Eleanor data products, where blends and systematic effects are already taken into account. To rule out the effect of contamination by other possible sources within the aperture or pixel, we overplotted the optimal apertures over Gaia sources 5 mag fainter than the targets. According to the magnitude–flux relation defined as $m_i - m_j = -2.5\log_{10}(b_i/b_j)$, where m_i and m_j are apparent magnitudes and b_i and b_j are fluxes, we thus assumed that a star that is 100 times fainter than the target has a negligible blend or modulation effect on the light curves and pulsations of the target(s). By examining the pixel-to-pixel light curves and the overlaid plots, we rule out possible effects of blends and either accept or reject the pre-identified eclipses and pulsations as genuine. On the other hand, independent pulsations could be matched directly with the stars within the TESS pixel using another Python module, called TESS-Localize (Higgins & Bell 2023). In this case, individual pulsations are traced to their origin within the TESS target pixel file. A signal with a periodogram peak that exceeds 7.5 times the average local noise level in the periodogram can be localized. This latter approach was only considered in situations where it becomes ambiguous to decipher, from the former, where the pulsations come from. As pointed out earlier, we only considered a few dominant peaks, which were used for the purpose (where necessary). In cases where the peaks were traced to neighboring stars, more pulsation frequencies of the star were extracted and subjected to a similar procedure using TESS-Localize until the target was established or disproved to have pulsations.

To ensure that the stars in the sample of pulsators are within the mass range suitable for the observed photometric variability, we placed them in the H-R diagram shown in Figure 3, using the information available in the literature. We plotted the luminosity, L, as the ordinate and the effective temperature, $T_{\rm eff}$, as the abscissa. The luminosity is computed using the equation $\log(L/L_\odot) = 0.4 \times (4.74 - M - BC)$, where $M = m - 5 \times \log(1000/\pi) + 5 - A_0$, BC is the bolometric correction, m is the apparent magnitude in the V band, π is the parallax, and A_0 is the interstellar extinction. π is obtained from the Gaia DR3 catalog (Gaia Collaboration et al. 2016, 2023). $T_{\rm eff}$ is the effective temperature from Gaia DR3, using the hot-star pipeline and obtained together with A_0 from this source. The bolometric correction is calculated in line with Flower (1996). The theoretical evolutionary tracks are also computed for the masses 4, 5, 6, 8, 10, 12, 15, 20, and $25M_\odot$ with the Warsaw–New Jersey evolution and pulsation code (described, for instance, by Pamyatnykh et al. 1998) using $Z = 0.012$, $X = 0.700$, and $v \sin i_{\rm ZAMS} = 100$ km s^{-1}. The theoretical instability strips are assigned using the same conditions (Pamyatnykh 1999). We see relatively good agreement of the positions of the stars on this diagram with the β Cep instability strip, but with the caveats that the external uncertainties of the Gaia DR3 hot-star effective temperatures are not well known and that our targets are binary systems, i.e., the measured temperature is a weighted average of the temperatures of both components.

To compute the ephemerides of the sample of pulsating stars, period analysis was conducted. We computed the preliminary orbital periods of the systems using the box-fitting least-squares

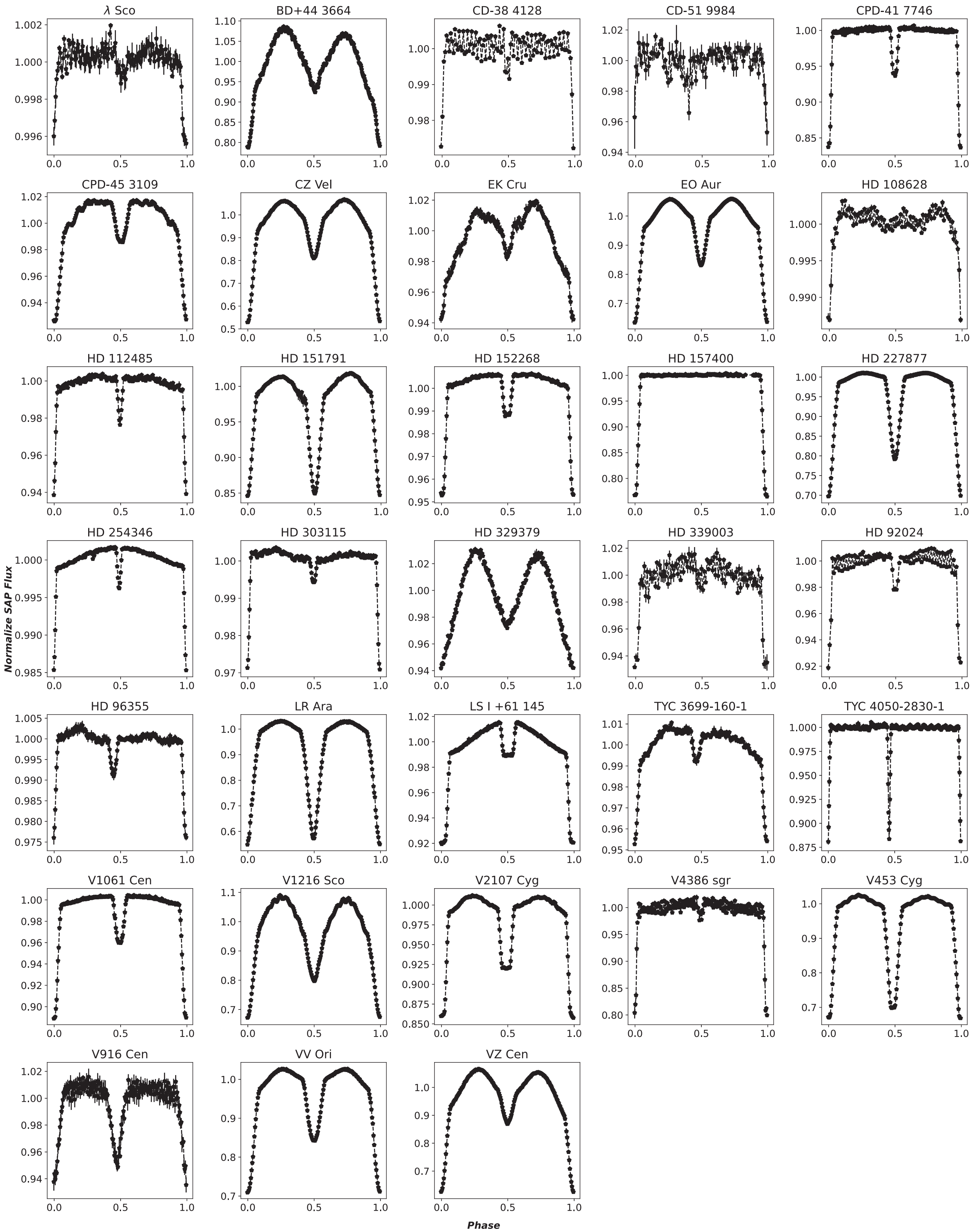

Figure 4. Binned phase diagrams of light curves of the β Cep pulsators in eclipsing binaries after prewhitening the strongest pulsations.

(Kovács et al. 2002) and Lomb–Scargle (Scargle 1982) periodograms incorporated in the lc-periodogram solver of the PHOEBE 2 program (Prša et al. 2016). The precision of the period obtained with the PHOEBE Estimator may improve during the detailed modeling of the light curves of the individual stars by applying the PHOEBE Optimizer and emcee, which is beyond the scope of this paper. Consequently, the estimated periods obtained from PHOEBE or available in the literature were used as input priors for the fitting of the orbital harmonic model and further refined during prewhitening using *Period04*. Harmonics that have amplitudes that satisfy the same S/N criteria as the pulsations were used to build the

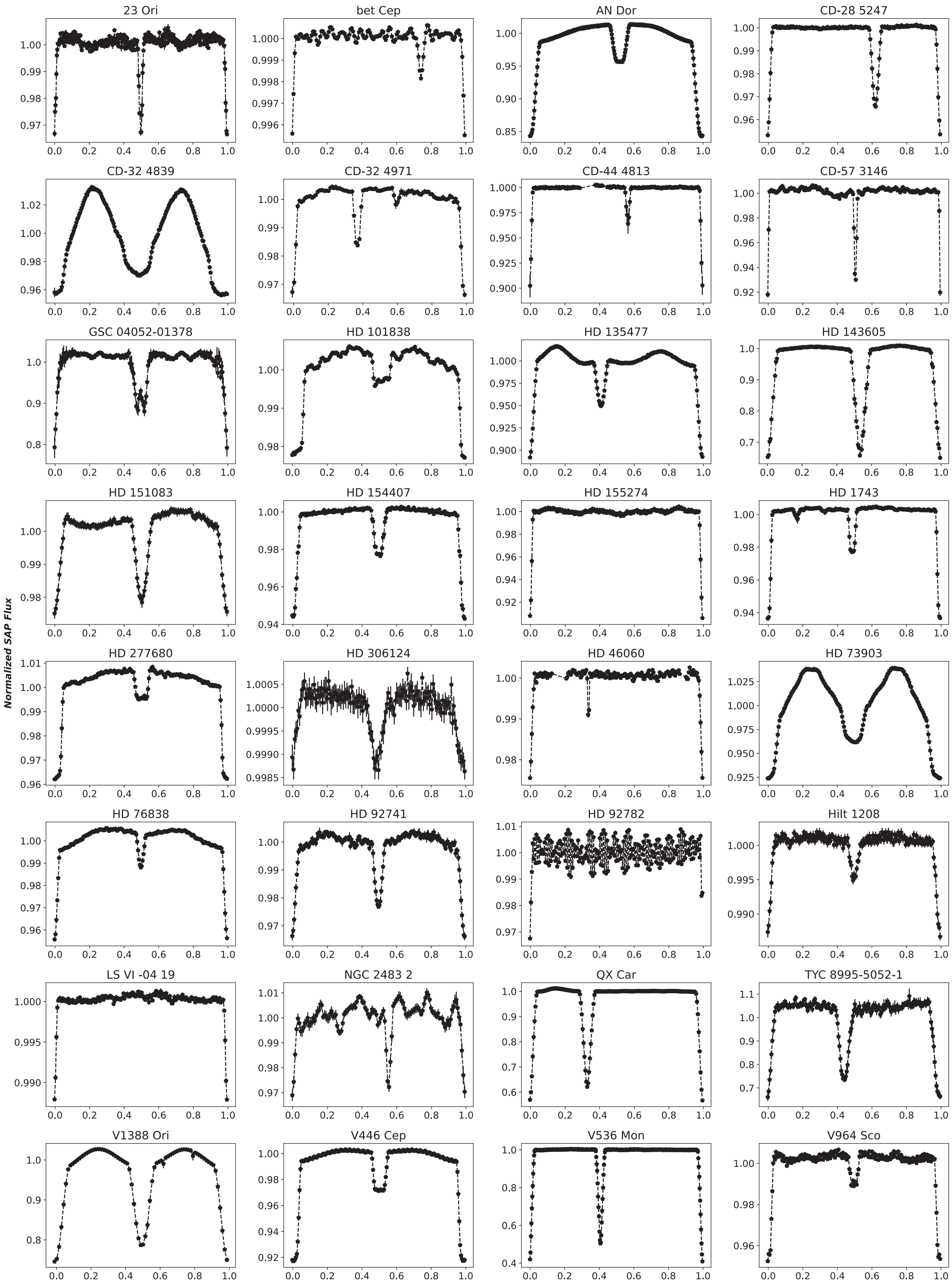

Figure 5. Binned phase diagrams of light curves of the candidates for β Cep pulsators in eclipsing binaries after prewhitening the strongest pulsations.

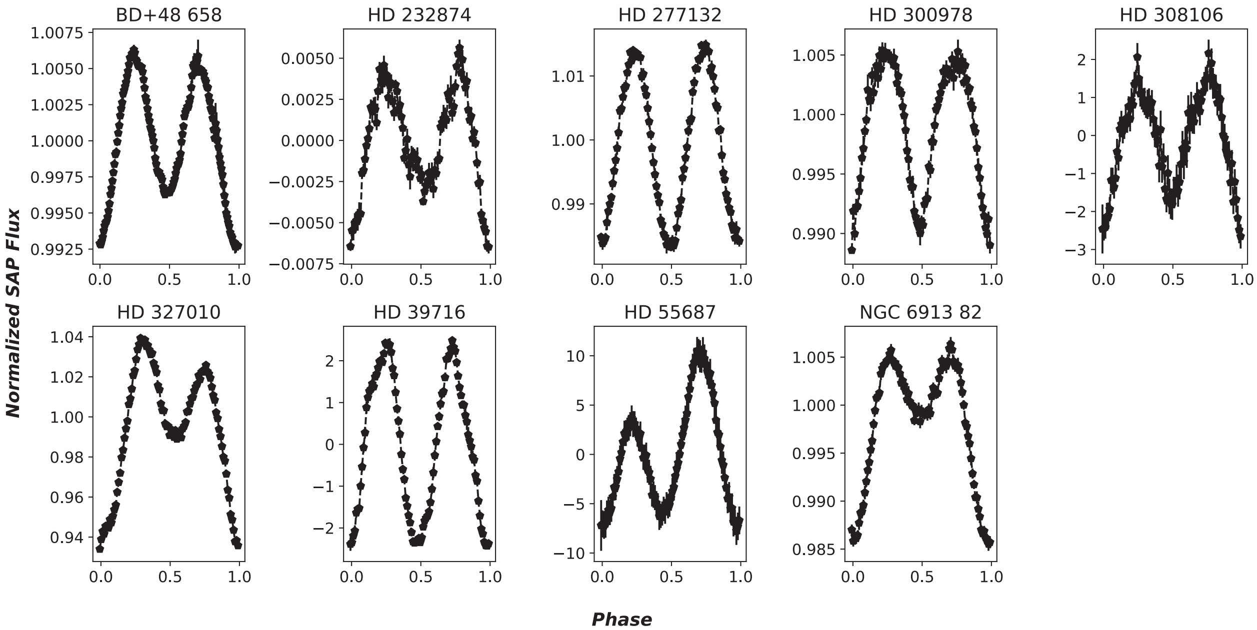

Figure 6. Binned phase diagrams of light curves of the ellipsoidal variables with β Cep pulsating component(s) after prewhitening the strongest pulsations.

orbital harmonic binary model. The periods reported in Tables 1–4 for the stars are the final periods obtained in the *Period04* program and that fit the orbital binary model the best.

4. Results and Discussion

4.1. Classification of Pulsators

Here we present the results of the analysis of the TESS photometry of 8055 stars. We report a total of 78 binary systems, of which we classify 43 as definite eclipsing binaries containing β Cep pulsators; a further 35 systems are listed as candidates that need further confirmation. There are also 10 possible ellipsoidal variables with pulsating components in our sample. The full lists of the definite β Cep pulsators and pulsating candidates as well as the ellipsoidal variables with their orbital ephemerides are shown in Tables 1–3. Table 1 shows the list of definite β Cep pulsators in eclipsing binaries. Stars with some unresolved blends and weak pulsations for which we were unable to unambiguously pinpoint the sources of the pulsations and/or eclipses are listed as eclipsing β Cep candidates and are shown in Table 2. Table 3 lists possible ellipsoidal variables with β Cep pulsating component(s). Objects that may appear to be β Cep pulsators in eclipsing binaries but according to our analyses are not are shown in Table 4. Stars that were rejected at the early stage of the analysis for conspicuously showing neither eclipses nor β Cep pulsations are not included in Table 4. The phase diagrams of light curves and the Fourier spectra of the residuals after subtracting the orbital light variations from the light curves of the stars in Tables 1–3 are shown in Figures 4–9, respectively. The phase diagrams of stars with incomplete ephemerides or insufficient data to give reliable phased light curves were not included in Figures 4–6.

The sample of pulsators also contains stars whose photometric variability had been previously identified in the literature. 16 Lac (Jerzykiewicz 1980), HD 101838, V4386 Sgr, and V916 Cen, which have been previously identified as β Cep stars in eclipsing binaries (e.g., Pigulski & Pojmański 2008; Chen et al. 2022), are corroborated by TESS photometry. Several others, such as HD 339003 and HD 344880, which were discovered to be β Cep stars in eclipsing binaries in the KELT project by Labadie-Bartz et al. (2020), and λ Sco, from space- and ground-based data (Bruntt & Southworth 2008; Handler & Schwarzenberg-Czerny 2013), are also corroborated by the TESS photometry. Further findings in the literature using the TESS data that are corroborated by the results of the analysis in this paper include: V453 Cyg (Southworth et al. 2020), VV Ori (Southworth et al. 2021), V446 Cep, HD 76838, and HD 227877 (Chen et al. 2022), AN Dor, EO Aur, HQ CMa, QX Car, V446 Cep, and V2107 Cyg (Southworth & Bowman 2022a), and V1388 Ori (Southworth & Bowman 2022b). The stars CD-38 4128, HD 303115, and Hilt 1208 have recently also been reported by Shi et al. (2024).

However, some stars that were previously rejected are accepted in this paper. HD 254346, for instance, which was rejected by Labadie-Bartz et al. (2020), owing to blending with the δ Scuti pulsator HD 43385, 112″ away, is accepted as a β Cep star, as we concluded that both HD 254346 and HD 43385 are pulsators, with the former being a β Cep star. HD 329379, which was classified as an ellipsoidal variable with pulsating components by Steindl et al. (2021), is reclassified in this paper as a β Cep pulsator in an eclipsing binary with some ellipsoidal variations.

On the other hand, LS CMa, HD 217919, FZ CMa, and η Ori, which were classified as β Cep candidate/definite pulsators in an eclipsing binary by Southworth & Bowman (2022a), and V Pup (Budding et al. 2021) have been dropped as β Cep pulsators in this paper. The single pulsation frequency of LS CMa is in the domain of SPB rather than β Cep pulsations. The pulsations of HD 217919 appear in groups of harmonically related signals, with the basic frequencies in the SPB domain. Hence, we do not regard the higher-frequency signals to be intrinsic (see Kurtz et al. 2015). FZ CMa appears to be a related case, with its pulsation spectrum dominated by a 2.7 day^{-1} signal and possible harmonics and subharmonics. Also, the masses derived for the components of FZ CMa by Southworth

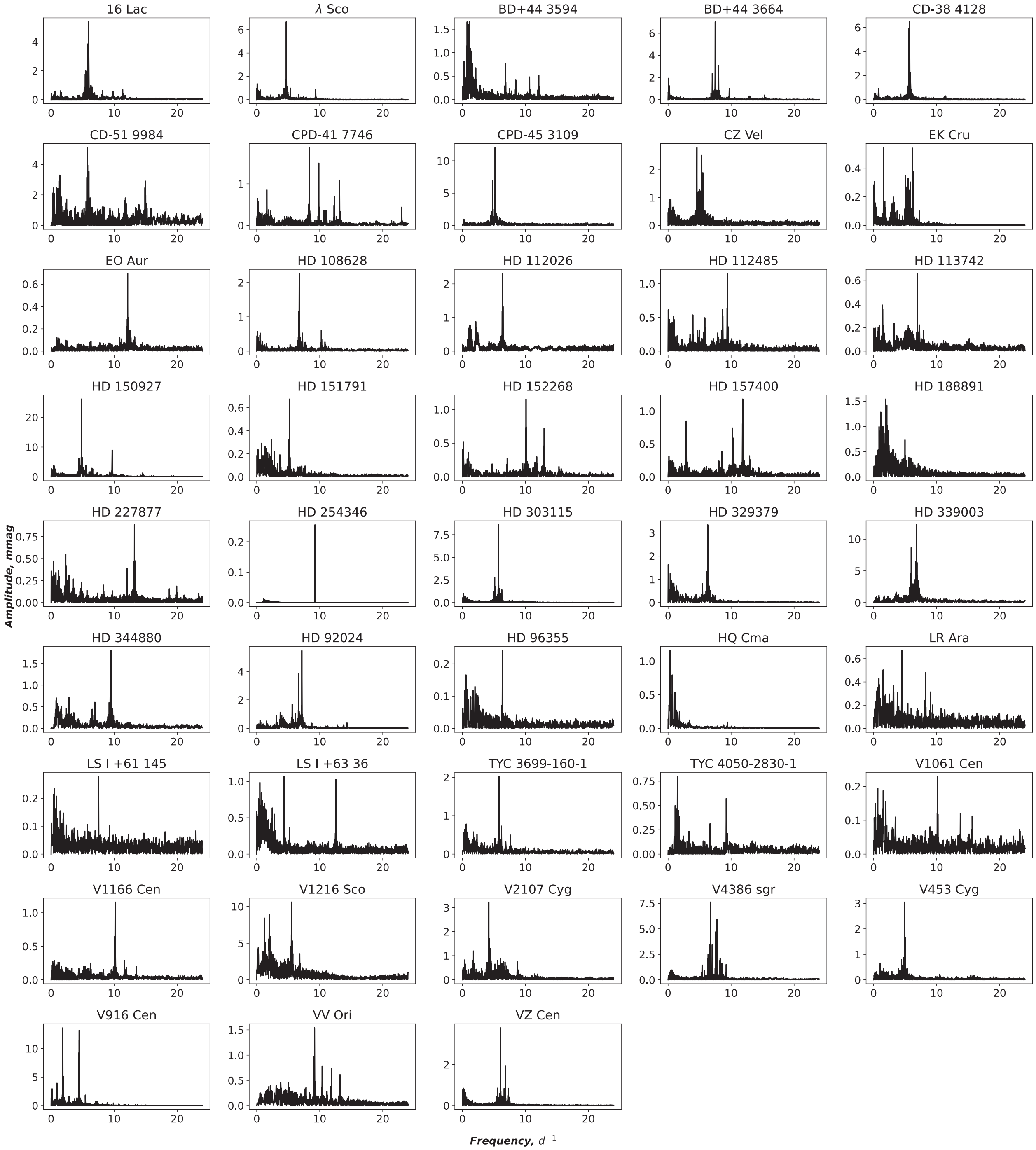

Figure 7. Fourier spectra of the definite β Cep pulsators in eclipsing binaries after removing the orbital light variations.

& Bowman (2022a) are around five times the solar mass, which is too low for β Cep stars. There are stochastic light variations present in the light curves of V Pup and possible instrumental effects (saturation), but no coherent periodic variability apart from the eclipses was found. CW Cep (Lee & Hong 2021) is classified by us as a gravity-mode pulsator (see the Appendix). The eclipse-removed light curves of η Ori show only a single frequency near 2.31 day^{-1} and its first harmonic. We therefore reject it as a β Cep pulsator.

In addition, several other objects (e.g., HD 277860) that have previously been identified as eclipsing binaries (e.g., IJspeert et al. 2021) or β Cep pulsators (e.g., Hilt 1208; Labadie-Bartz et al. 2020) are only now reported to show both types of variability. A brief discussion of each of the pulsators is given in the Appendix.

A number of stars that were previously classified as β Cep pulsators in eclipsing binaries, but have spectral types outside the range defined by our selection criteria or have not been observed by TESS at the time of this work, are not captured in detail in this analysis. These stars include CD−44 4484—identified as a β Cep candidate in an eclipsing binary by Labadie-Bartz et al. (2020), who recommended reanalysis of the target to confirm or disapprove it, owing to their observation of shallow eclipses; V447 Cep—identified as a β

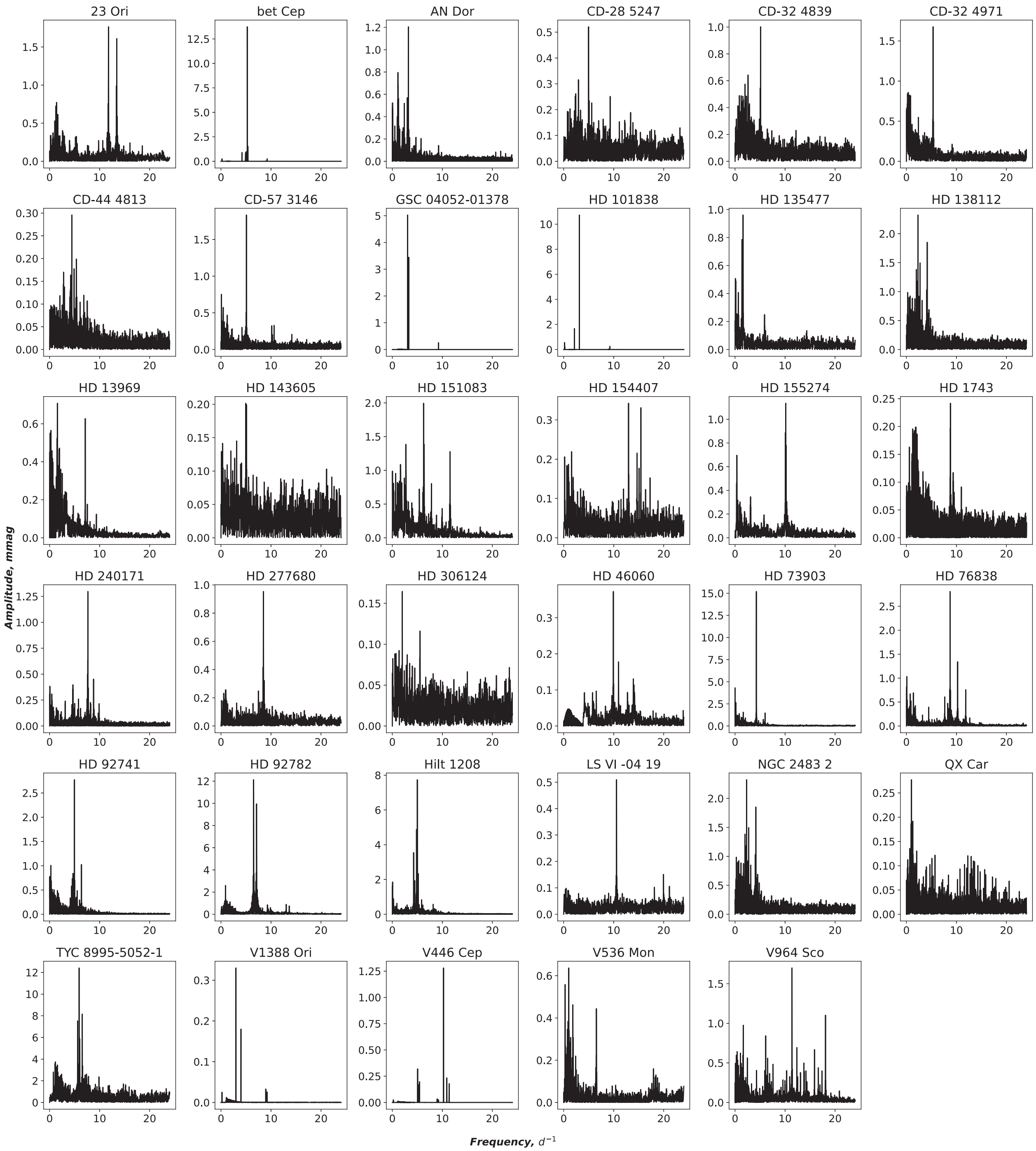

Figure 8. Fourier spectra of the candidates for β Cep pulsators in eclipsing binaries after removing the orbital light variations.

Cep by Stankov & Handler (2005) and an eclipsing binary by Labadie-Bartz et al. (2020); CD−46 4432—previously identified as a β Cep pulsating candidate, but rejected by Labadie-Bartz et al. (2020); and HD 168050—identified as a β Cep in an eclipsing binary by Pigulski & Pojmański (2008), but has not been observed by TESS. Following a more curious look at these targets, CD−44 4484, which has a spectral type B5, appears to be an eclipsing binary with β Cep pulsating component. V447 Cep turns out to be an eclipsing binary with ellipsoidal variations of different period, but no pulsations. CD −46 4432, which was rejected and its variability attributed to CD−46 4437 by Labadie-Bartz et al. (2020), appears to be the one pulsating instead. However, it has a spectral type of B5 and is beyond the spectral range analyzed in this paper.

The number of confirmed β Cep pulsators in eclipsing binaries has so far been fairly small (<30). Using TESS photometry, 78 definite and candidate β Cep pulsators in eclipsing binaries have been reported in this work, of which 43 are adjudged definite and 35 candidate β Cep pulsators, respectively. Nineteen of the 78 pulsators have already been previously identified in literature as β Cep pulsators in eclipsing binaries, 23 have been identified as eclipsing binaries only, and seven have been identified as β Cep pulsators only. This results in 59 new discoveries in this work,

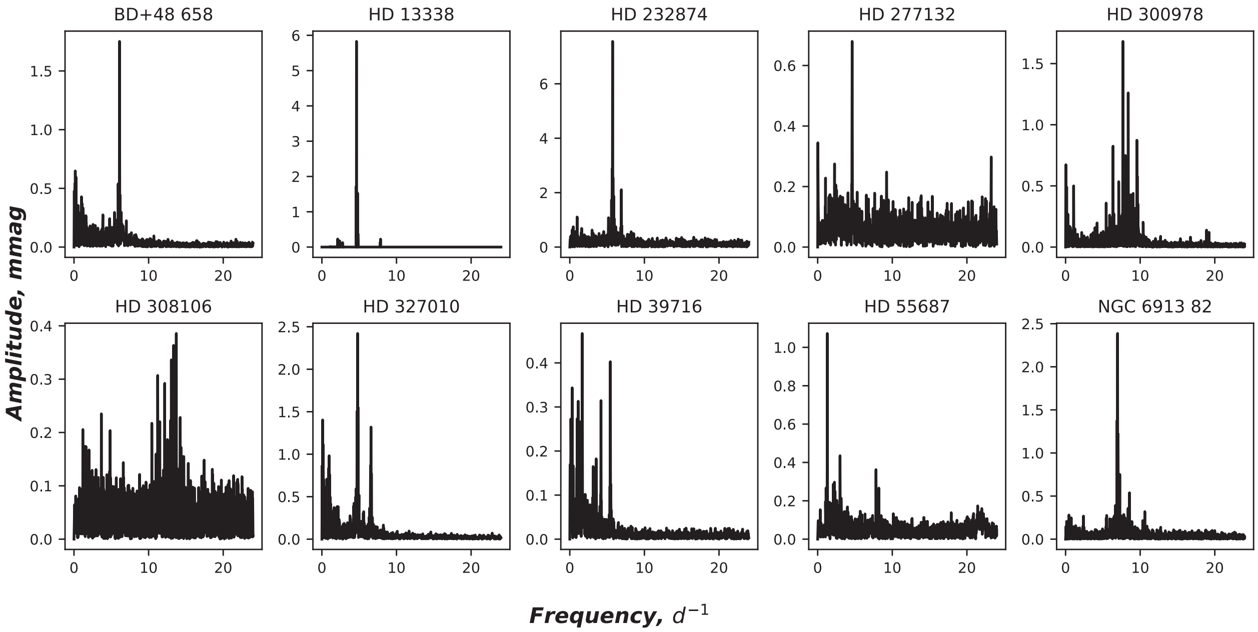

Figure 9. Fourier spectra of the likely ellipsoidal variables with β Cep components after removing the orbital light variations.

in which both variabilities (eclipsing binary and β Cep pulsation) are newly identified in 29 systems and single variabilities (eclipsing binary or β Cep pulsation) are newly identified in 30 stars. Ten ellipsoidal variables with β Cep pulsating components are also identified in this work, with their β Cep variability newly identified in eight of the 10.

4.2. Periodicities of the Pulsators

The orbital periods of the stars and their analytical uncertainties are given in Tables 1–4. Orbital periods available in the literature or obtained with the PHOEBE Estimator (Prša et al. 2016) are used as inputs for the fitting of the harmonic model and the estimation of precise orbital period using *Period04* (Lenz & Breger 2005) during prewhitening. Where there are already established precise periods in the literature, we adopted them after checking their validity for the times of the TESS observations. The validity of the orbital period values was checked by comparison with a multi-harmonic fit to the orbital light curves optimized within *Period04*. For stars with incomplete orbital cycles in the 30 minutes light curve (i.e., light curves with only the primary eclipse visible and with gaps between the consecutive primary eclipses), we determined the periods with the 2 minutes cadence light curves, if available. In the QLP data, sections of data that are present in the 2 minutes SPOC data are sometimes missing. Where there is no light curve with a complete orbital cycle in both cadences (2 minutes SPOC and QLP data) a lower limit to the period is adopted. The analytical uncertainties of the periods were estimated using the *Period04* program. We obtained an orbital period range of 1.4074–161.25 days for our sample of pulsators of 78 definite and candidate β Cep pulsators. However, more than 80% of the sample has orbital periods below 20 days.

Period changes and modulations are usually examined via eclipse timings and observed-minus-calculated ($O-C$) diagrams. However, the time spans of the TESS data, which are in most cases only one or two months, make it unreliable to compute them, as they are too short to show any period change. As a result, the eclipse timings and $O-C$ diagrams are not computed. Nevertheless, we computed the epochs of the binary light curve by estimating the time of the minimum (i.e., the midpoint) of the primary eclipse, which in binary star analysis can also be referred to as the time of superior conjunction (t_supconj). We arrived at the epochs by manually zooming into the primary eclipses and reading off the midpoint of the eclipse curve. The errors were estimated visually on a case-by-case basis and are thus upper limits to the real error.

5. Conclusion

In this paper, we have conducted a search for β Cep pulsators in eclipsing binaries in a sample of 8055 stars of spectral type B0–B3 using the TESS QLP and 2 minute cadence data. The results of the photometric and pulsation analyses indicate a total of 78 pulsators in eclipsing binaries, of which 43 are recognized as definite and 35 are candidate pulsators, after accounting for blends and the removal of false positives. We computed the orbital ephemerides and tabulated the dominant pulsation frequencies with their amplitudes and S/Ns. We further crossmatched our results with the results of previous searches. Among the 78, 59 are new discoveries, as 19 have been previously identified as β Cep pulsators in eclipsing binaries. Twenty-three stars have also been previously identified as eclipsing binaries only and seven have been previously identified as β Cep pulsators only. The number of pulsators in our sample accounts for about 1% of the sample and contributes about 59 new definite β Cep pulsators and candidates in eclipsing binaries to the pool already discovered to date. There are also 10 possible ellipsoidal variables with pulsating components in our sample. This work provides a bigger sample for a more general and homogeneous in-depth asteroseismic analysis of β Cep pulsators. It will provide the needed constraints to better calibrate the internal mixing profile and possibly resolve the mass discrepancy in massive stars via the combined strengths of binary and asteroseismic modeling.

Acknowledgments

This work was supported by the Polish National Science Center (NCN) under grant No. 2021/43/B/ST9/02972. This paper used TESS data obtained from the Mikulski Archive for Space Telescopes (MAST) at the Space Telescope Science Institute. The observations analyzed for the stars in Tables 1–4 in the paper can be accessed via doi:10.17909/8rpk-re37. Support for MAST for these data is provided by the NASA Office of Space Science via grant NAG5-7584 and by other grants and contracts. Funding for the TESS mission is provided by the NASA Explorer Program. This paper also made use of the SIMBAD database and the VizieR catalog access tool, operated at CDS, Strasbourg, France; and the SAO/NASA Astrophysics Data System. It has also made use of data from the European Space Agency (ESA) mission Gaia (https://www.cosmos.esa.int/gaia), processed by the Gaia Data Processing and Analysis Consortium (DPAC; https://www.cosmos.esa.int/web/gaia/dpac/consortium). Funding for the DPAC has been provided by national institutions, in particular the institutions participating in the Gaia Multilateral Agreement. We also thank the referee for the invaluable constructive review and recommendations that helped to improve the paper.

Facility: TESS

Software: Python, Period04 (Lenz & Breger 2005), Eleanor (Feinstein et al. 2019; Brasseur et al. 2019; Burke et al. 2020), TESS-Localize (Higgins & Bell 2023).

Appendix
Short Remarks on Individual Stars

A.1. β Cep Pulsators in Eclipsing Binaries

16 Lac = TIC 129538133. This was discovered to be a spectroscopic binary by Lee (1910), a pulsating star by Walker (1951), and an eclipsing binary by Jerzykiewicz (1980). Detailed studies of the star to determine its orbital and absolute parameters have been undertaken by a number of authors (e.g., Lehmann et al. 2001; Southworth & Bowman 2022a). An asteroseismic analysis of the pulsating component was conducted by Thoul et al. (2003).

λ Sco = TIC 465088681. This is a multiple system with an inner eclipsing binary and a tertiary component. The inner eclipsing binary is composed of a B star of 10.4 ± 1.3 solar mass, showing β Cep pulsations, and a 1.6–2.0 solar mass unresolved main-sequence star (Southworth & Bowman 2022a). Detailed analyses of the system can be found over a wide range of papers (e.g., De Mey et al. 1997; Handler & Schwarzenberg-Czerny 2013).

BD+44 3594 = TIC 353099086. This is a Be star (Jaschek & Egret 1982) with a long orbital period. Although it has a long-period variable candidate (2MASS J20490628+4525007) 59.″79 away, there is no indication of a significant blending effect. It shows both β Cep and SPB pulsations. The binarity and the pulsations are reported for the first time in this work.

BD+44 3664 = TIC 330081196. This star has its spectral type classified as B1Vn by Straizys et al. (1989). It is an eclipsing binary with β Cep pulsations and has some nearby Gaia sources that could contaminate the light curve. However, the CROWDSAP parameter (i.e., the crowding metric that reflects the fraction of the flux in the aperture that is due to the target itself, not the nearby sources) for this object is 0.89624, suggesting that the signals most likely originate from the target. The binarity and the pulsations are newly identified in this work.

CD−38 4128 = TIC 134522557. This star has no significant nearby contaminator. It has been observed in TESS sectors 6, 7, 34, 35, 61, and 62 using TESS camera 3. Whereas the binarity was first reported by Balona & Ozuyar (2020), its β Cep variability is newly reported in this work. There are still a number of pulsations left in its phase diagram shown in Figure 3.

CD−51 9984 = TIC 314529804. Classified as a B0.5III star in the spectral classification and photometry of southern B stars compiled by Feast et al. (1961). This star has a neighbor, TIC 314529900, which is 1 mag brighter, at 76.″18 from it, and claimed to be an eclipsing binary star (IJspeert et al. 2021). The available TESS photometry of the latter star does however not show any eclipses. Therefore, we suggest that the eclipses and pulsational signals we observed emanate from CD−51 9984. However, its β Cep variability was first identified by Balona & Ozuyar (2020).

CPD−41 7746 = TIC 339570153. There are many faint nearby sources within the aperture mask (e.g., 2MASS J16542911-4139115). However, the CROWDSAP parameter for this object is 0.89506, suggesting that the variability signals most likely originate from the target.

CPD−45 3109 = TIC 28957011. This star has no nearby contaminant. The binarity and the pulsations are reported for the first time in this work.

CZ Vel = TIC 355656323. This was classified as an eclipsing binary by Dvorak (2004). The pulsations are reported here for the first time.

EK Cru = TIC 379012185. This was identified as an eclipsing binary by Otero & Wils (2005). The pulsations (both of the SPB and β Cep type) are reported here for the first time.

EO Aur = TIC 408937625. This was discovered to be eclipsing by Gaposchkin (1943) and to be a β Cep pulsator by Southworth & Bowman (2022a). It contains two early B stars (Southworth & Bowman 2022a) in a 4.06550(3) days orbit.

HD 108628 = TIC 450918869. This was discovered to be a β Cep pulsator by Pigulski & Pojmański (2008). These authors, however, treated it as an isolated single star, as no eclipses seem to have been detected by them. However, the TESS QLP light curve shows primary eclipses of 18 mmag depth.

HD 112026 = TIC 436382800. Although there is a nearby star, TIC 436373277 = HD 312121, which could possibly modulate the light curve, the pulsational signals we observed are traced to HD 112026. The CROWDSAP parameter for the target is also 0.96683, and the amplitude of the dominant pulsation is 2.22 mmag. The orbital period of some 43.205 (9) days is rather long and the orbit is clearly eccentric. The binarity and the pulsations are reported for the first time in this work.

HD 112485 = TIC 437617380. This was identified as an eclipsing binary in the catalog of OBA-type eclipsing binaries observed by TESS compiled by IJspeert et al. (2021). Our analysis suggests that there is no significant contamination from TIC 437612835, which is an A0 star 89.″69 away.

HD 113742 = TIC 440817830. This star has a relatively long orbital period of 15.68844(8) days and an eccentric orbit. There is a nearby G3V star, with a similar TESS magnitude, at 106.″85 from it. However, our blending analysis suggests that the detected light variations come from HD 113742. The eclipses and pulsations are reported for the first time here.

HD 150927 = TIC 78636551. This was discovered to be a β Cep variable by Pigulski & Pojmański (2008). The TESS light curves imply the presence of eclipses, with depths of about 0.04 mag and a 14.33(2) days period within the high-amplitude pulsations (the orbital period could be that or twice that value). The dominant pulsation frequency of 4.84325(2) day^{-1} appears to be within an unresolved multiplet, hence our determination of its amplitude is uncertain (but in relatively good agreement with Pigulski & Pojmański 2008).

HD 151791 = TIC 246552414. Two stars (SAO 227312 and TYC 7880-2706-1), which are about 2.5 mag fainter than the target, are found within 36″ from the target. Our blending analysis suggests that the signals are consistent with location of the brightest star, but not uniquely so. The star 36″ away also seems to be a hot pulsating star. The eclipses and pulsations are reported for the first time here.

HD 152268 = TIC 339680203. This was also identified as an eclipsing binary in the catalog of OBA-type eclipsing binaries observed by TESS compiled by IJspeert et al. (2021). Its β Cep variability is, however, newly identified in this work.

HD 157400 = TIC 158688754. This star has no nearby contaminant. The binarity and the pulsations are reported for the first time in this work.

HD 188891 = TIC 171502734. The catalog of Kepler eclipsing binaries (Kirk et al. 2016) lists this system with a period of 161.25 days. Pulsations are present at very low amplitude in both the SPB and β Cep frequency regions, both in the Kepler and TESS data.

HD 227877 = TIC 91111448. This was discovered to be eclipsing by IJspeert et al. (2021) and to be a β Cep pulsator by Chen et al. (2022). However, its orbital period was not computed by these authors. We obtained a period of 1.70664(4) days for the system.

HD 254346 = TIC 426520557. This was rejected by Labadie-Bartz et al. (2020) as a β Cep pulsator, owing to blending with the δ Scuti pulsator HD 43385, 112″ away from it. However, it is accepted as a β Cep in this paper, as the TESS photometry allows us to conclude that both HD 254346 and HD 43385 are pulsators, with the former being a β Cep star.

HD 303115 = TIC 458263480. There are many faint sources in the field 7 mag fainter than the target in the G band, with the closest at 70.″19. Our analysis of possible contamination suggests that both the eclipses and the pulsations come from the target.

HD 329379 = TIC 122314621. Steindl et al. (2021) classified this as an ellipsoidal variable that also shows pulsations. We suggest those to be of the β Cep type. The pulsation amplitudes are enhanced near the ellipsoidal light minima, suggesting interplay between the pulsations and tidal forces. A phase diagram of the pulsation-removed orbital light curve shows the presence of shallow eclipses.

HD 339003 = TIC 10891640. This was discovered to be a β Cep pulsator in an eclipsing binary by Labadie-Bartz et al. (2020), who also noticed a reflection effect in the light curve. This is corroborated by the TESS photometry.

HD 344880 = TIC 451932686. This star was also discovered to be a β Cep pulsator in an eclipsing binary by Labadie-Bartz et al. (2020), which is confirmed by our analysis of its TESS photometry. It has a long orbital period of 54.49399(1) days.

HD 92024 = TIC 458076434. This is a known β Cep pulsator in an eclipsing binary, e.g., see Freyhammer et al. (2005).

HD 96355 = TIC 466528132. This was also discovered to be an eclipsing binary by IJspeert et al. (2021), in their catalog of OBA-type eclipsing binaries observed by TESS. A source, TYC 8958-3680-1, which is 4.1 mag fainter than the target in the TESS band, is at 38.″58 from it. However, the pulsational signals appear to originate from HD 96355.

HQ CMa = TIC 106830354. This was discovered to be eclipsing by Jerzykiewicz & Sterken (1977) and as a β Cep and SPB candidate by Southworth & Bowman (2022a). The orbital period is unknown, as there is no agreement in the literature about it. Sterken et al. (1985) reported an orbital period of 24.6033 days, whereas Southworth & Bowman (2022a) reported a period range of 21.2–22.6 days or 34.5 days or longer. In this work, we also could not unambiguously determine this period. Pulsations are found in both the SPB and β Cep frequency domains.

LR Ara = TIC 447530589. This star was cataloged as an eclipsing binary by Brancewicz & Dworak (1980). Although there is a contaminator, UCAC4 143-192850, 31.″26 away, which is about 3 mag fainter, there is no indication that the signals come from the contaminator: the eclipses are too deep to be caused by blending with this star, which is also too cool to pulsate with the observed periods. Pulsations (of both the SPB and β Cep types) are reported here for the first time.

LS I+61 145 = TIC 406965391. This was also identified as an eclipsing binary in the catalog of OBA-type eclipsing binaries observed by TESS compiled by IJspeert et al. (2021). Its β Cep variability is, however, newly identified in this work.

LS I+63 36 = TIC 359042331. A faint star, TIC 359042198, with a magnitude difference of 4.86 in the G band is 109.″94 away from the target. The TESS light curves of TIC 359042331 show a primary eclipse depth of 34.5 mmag, a secondary eclipse depth of 18 mmag, and an amplitude of the dominant pulsation of 1.05 mmag. Considering the magnitude difference between the stars, it is unlikely that the contaminator caused signals of such amplitude. We therefore conclude that both the eclipses and pulsations originate from TIC 359042331.

TYC 3699-160-1 = TIC 245470639. Both β Cep and SPB pulsations as well as a reflection effect are present. A star (TYC 3699-874-1) 0.3 mag fainter than the target in the TESS band at 69.″89 distance is present, but both the β Cep pulsations and the eclipses arise from the target.

TYC 4050-2830-1 = TIC 458879750. There is no nearby contaminator bright enough to significantly modulate the light curve. Both β Cep and SPB pulsations are present.

V1061 Cen = TIC 334443373. Otero (2003) classified this as an eclipsing binary. The pulsations are reported here for the first time.

V1166 Cen = TIC 443262289. This was first classified as an eclipsing binary by Alfonso-Garzón et al. (2012) and corroborated by IJspeert et al. (2021) in their catalog of OBA-type eclipsing binaries observed by TESS. The pulsations are reported here for the first time.

V1216 Sco = TIC 247315421. This was identified as an eclipsing binary by Otero (2003). The pulsations are reported here for the first time.

V2107 Cyg = TIC 42244951. This was also discovered to be an eclipsing binary by Kazarovets et al. (1999), using Hipparcos satellite data, and as a β Cep pulsator by Southworth & Bowman (2022a). Rotational splitting and tidally perturbed modes are also suspected by the latter authors.

V4386 Sgr = TIC 60433558. This was first discovered to be eclipsing by Pigulski & Pojmański (2008), corroborated by Avvakumova et al. (2013), and also as a β Cep pulsator by Pigulski & Pojmański (2008), corroborated by Chen et al. (2022).

V453 Cyg = TIC 90349611. This eclipsing system has an orbital period of 3.8900(4) days, an eccentric orbit, and exhibits apsidal motion (Wachmann 1973). Its β Cep pulsations were analyzed by Southworth et al. (2020), who also reported tidally perturbed pulsations in the system.

V916 Cen = TIC 322078735. This star was discovered to be a β Cep pulsator in an eclipsing binary with an orbital period of 1.4632361(21) days by Pigulski & Pojmański (2008). The TESS photometry in this analysis confirms its variability type. It is also a Be star (Moffat & Vogt 1975), a member of the open cluster Stock 14, and it shows other types of variability related to γ Cas and λ Eridani (Pigulski & Pojmański 2008). Although there could be significant third light contribution, the amplitude of the dominant β Cep pulsation is reasonably large (13.2 mmag), so we cannot conclude that it originates from the modulation of light curves by the contaminating light.

VV Ori = TIC 50897998. This was discovered to be an eclipsing binary with a β Cep primary and an SPB secondary by Southworth et al. (2021). These authors also observed a changing orbital inclination, which was adjudged to be driven by its dynamical interactions with a third body. This system was also among the five β Cep pulsators identified by Chen et al. (2022).

VZ Cen = TIC 304803692. This was first identified as an eclipsing binary by Alfonso-Garzón et al. (2012). The pulsations are reported here for the first time.

A.2. Candidates for β Cep Pulsators in Eclipsing Binaries

23 Ori = TIC 264592553. This star was first identified as a spectroscopic binary by Eggleton & Tokovinin (2008) and as an eclipsing binary by IJspeert et al. (2021). In this work, we newly identify β Cep variability in this system. However, whereas the pulsations originate from 23 Ori, it is not clear whether the eclipses seen in the light curve come from it or from HD 35148, 32″ apart from the target.

β Cep = TIC 321818578. This has been studied extensively as a single star (Shibahashi & Aerts 2000; Bowman et al. 2022), as none of the authors had observed eclipses in its light curve. However, the TESS photometry shows shallow eclipses of 10 mmag in the QLP data and 20 mmag in the sector 58 data, for instance. It is not certain that the eclipses involve the pulsating star. They could possibly come from β Cep B, which is 13.″38 from it, with a V magnitude of 8.63.

AN Dor = TIC 220430912. AN Dor was first discovered to be an eclipsing binary by Kazarovets et al. (1999), using the Hipparcos satellite, and was cataloged as a variable B star in an eclipsing binary by Percy & Au-Yong (2000), who pointed out that the short-term variability is uncertain. Southworth & Bowman (2022a), using TESS data, reported a total eclipse and a strong reflection effect, and also observed SPB and β Cep pulsations over a wide frequency range of 1–4 day^{-1} for dominant pulsations. We concur with this finding, with the caveat that we cannot confidently rule out the variations in the β Cep frequency domain being due to combination frequencies of the SPB pulsations.

CD−28 5247 = TIC 130348163. This has weak pulsations and blends (among others) with TIC 130348237, which could be the origin of the pulsational signals.

CD−32 4839 = TIC 144535458. We detected ellipsoidal light variations and shallow eclipses. There is a single possible β Cep pulsation mode, but given the presence of nearby sources (e.g., Gaia DR2 5547616364978530 56, 3.858 mag fainter than the target in the G band, 50″ away, and TYC 7125 2876-1, 0.03 mag fainter than the target in the B band, 112.″32 away), we cannot be sure that they arise in the photometric binary.

CD−32 4971 = TIC 145760541. This star is an optical triple system and located in a crowded field. We cannot safely conclude that both the pulsational signals and the eclipses arise from one and the same object.

CD−44 4813 = TIC 28699677. This star has a long orbital period with weak pulsations that we cannot safely exclude as originating from some fainter star nearby.

CD−57 3146 = TIC 463899225. There are some blending issues with a few contaminators nearby. This object was discovered to be an eclipsing binary by IJspeert et al. (2021), in their catalog of OBA-type eclipsing binaries observed by TESS. The pulsations that are suspected to originate from the target are reported in this work for the first time.

GSC 04052-01378 = TIC 390515222. We cannot confidently exclude that the weak pulsational signal detected arises from one of the neighboring stars.

HD 101838 = TIC 321947833. Its variability was discovered by Pigulski & Pojmański (2008) and its β Cep pulsations by Drobek et al. (2010). It was shown that the orbital period could be about 5.41167 days or twice as much (Drobek et al. 2010). These authors, however, favored twice 5.41167 days, which could result in double eclipses of equal depths instead of a single eclipse with 5.41167 days. In this paper, an orbital period of 5.41187(7) days was obtained from the TESS light curve, from the S10, 11, 37, and 38 data. Also, the pulsation frequencies of the star are all below 3.2 day^{-1}, making us suspect this is in fact a rapidly rotating SPB and not a β Cep star.

HD 135477 = TIC 455667423. This was also identified as an eclipsing binary in the catalog of OBA-type eclipsing binaries observed by TESS compiled by IJspeert et al. (2021). The orbit is clearly eccentric. It has a faint long-period variable, about 4 mag dimmer, at 29″ from it. Our analysis suggests that the target has low-amplitude pulsations in both the SPB and β Cep frequency domains. As some (but not all) of the frequencies in the β Cep range can be explained with combinations of lower frequencies, we retain this system among the candidates instead of the firm detections.

HD 138112 = TIC 284374921. This was identified as an eclipsing binary in the catalog of OBA-type eclipsing binaries observed by TESS compiled by IJspeert et al. (2021). It has a few contaminators nearby. The four brightest contaminators in the TESS band are three red giants and one A-type star. The eclipses are shallow and the pulsations are weak, although in the β Cep domain.

HD 13969 = TIC 264613302. This star has a long orbital period of about 16 days and shallow flat-bottomed eclipses of about 0.02 mag depth. The CROWDSAP parameter is 0.90977 and the amplitudes of the pulsations are below 0.6 mmag. We thus cannot be sure that both the pulsations and eclipses come from the target.

HD 143605 = TIC 427406031. Although there is a long-period variable (2MASS J16041100-5625180) 80.″72 away (3.4 mag fainter than the target in the TESS passband), our blending analysis suggests that the signals emanate from HD 143605. The pulsation is of low amplitude, but significantly present in the data. However, its position in the theoretical H-R diagram with a mass of $5M_{\odot}$ makes us doubt whether it is a β Cep star. We could face an SPB pulsation shifted by rotation into the β Cep regime.

HD 151083 = TIC 51288359. This was classified as a Be star by Balona & Ozuyar (2021). The shape of the light curve resembles eclipses with a short period (1.8016(4) days or half its value), with pulsations superposed. The features reminiscent of eclipses cannot be fully distinguished from the beating of multiple pulsation modes.

HD 154407 = TIC 42424196. This is a visual double with TIC 42424192 that has almost identical basic stellar parameters. The pulsations and eclipses could thus arise from different objects, respectively, or from either of the two stars.

HD 155274 = TIC 45731009. This is 5.″71 away from another eclipsing binary, TIC 45731014, first identified by IJspeert et al. (2021). It is not clear where the variability observed in both comes from: either both are eclipsing binaries or one is modulated by the other. We cannot rule out IJspeert et al. (2021) misidentifying the source of the eclipses. Also, the Gaia source located at the coordinates of TIC 45731014, a red star, is more than 6 mag fainter than TIC 45731009.

HD 1743 = TIC 428415975. This was also classified as an eclipsing binary by IJspeert et al. (2021) in their catalog of OBA-type eclipsing binaries observed by TESS. However, it blends with the nearby pulsating star TIC 428415927, which is 4 mag fainter in the TESS passband. Given the low amplitude of the pulsations (0.18 mmag), this close-by star cannot be confidently excluded as their source.

HD 240171 = TIC 314034024. The amplitudes of the pulsation frequencies are similar to that of the suspected orbital variability, with a 5.1514(9) days period. The shape of the latter signal may be due to eclipses, although it appears rather reminiscent of a "heartbeat" star light curve. There are also nearby contaminators, such that we cannot clearly identify the origin of the signals.

HD 277680 = TIC 122883754. This was reported to be an eclipsing binary by IJspeert et al. (2021). However, it is sufficiently close to TIC 122883745 (6.″27), which is 2.3 mag fainter than the target in the TESS band, such that it is not clear where the signals come from. The eclipses are shallow (40 mmag), so the 6″ companion could be responsible, but the pulsations should come from the target, as this companion is too cool.

HD 306124 = TIC 466887289. Both the eclipses and the pulsational signals have very low amplitude. Hence we cannot exclude them originating from some of the fainter close-by stars.

HD 46060 = TIC 25041731. The signals could come from more than one star, as it blends with TIC 25041724 and TIC 25041738. It has a long orbital period of 20.6094(8) days.

HD 73903 = TIC 141497319. Jaschek & Egret (1982) classified it as a Be star. There are many bright nearby stars, including CPD−45 2774, so it is not clear where the signals come from.

HD 76838 = TIC 30562668. This was discovered to be eclipsing by IJspeert et al. (2021) and to be a β Cep pulsator by Chen et al. (2022), using TESS photometry. There are several bright early-type stars around this object, two classified in SIMBAD as eclipsing binaries. Although the nearest eclipsing binary to it is a faint Gaia source, the second (CD-42 4806), 46.″13 away, is only about 1 mag fainter. There is sufficient contamination that it is not clear whether HD 76838 is the source of the observed variability.

HD 92741 = TIC 458561474. This was also identified as an eclipsing binary in the catalog of OBA-type eclipsing binaries observed by TESS compiled by IJspeert et al. (2021). The target has nearby stars. Examples include CPD-59 2451 and CD−59 3219B, which are 2 and 4.8 mag fainter in the TESS band, at 45″ and 4.″49 from it, respectively, which could possibly have significantly modulated the light curve.

HD 92782 = TIC 458599043. There are two relatively bright stars, HD 92758 (A6/7 V) and HD 303139 (M0), of almost similar magnitudes in the V band in the neighborhood of the target (less than 100″ away). It is not clear whether both the pulsations and the eclipses originate from our target of interest. The phased eclipse light curve is somewhat asymmetric.

Hilt 1208 = TIC 269228628. This was first discovered to be a β Cep pulsator by Labadie-Bartz et al. (2020). However, these authors did not observe any eclipse in its light curve. The TESS photometry shows shallow eclipses of about 38 mmag depth. Whether that eclipse originates from it or is contributed by the Gaia source 88.″50 from it, with a magnitude difference of 5.71164 in the G band, is not yet established.

LS VI −04 19 = TIC 33091633. There is a nearby star, TIC 33091617, which cannot be excluded as the origin of the apparent pulsational signals. The brighter star, HD 52047, 1.′5 away from the target, is not.

NGC 2483 2 = TIC 129364361. This star is located in a dense field in an open cluster. The observed light curve is likely a superposition of the variability of several stars.

QX Car = TIC 469247903. This was discovered to be a spectroscopic binary by Thackeray et al. (1973), eclipsing by Cousins et al. (1969), and a β Cep candidate by Southworth & Bowman (2022a). It has an orbital period of 4.47800(2) days and a dominant pulsation frequency of 5.7216 day^{-1} at an S/N of 5.5. There is no significant contaminant in the aperture mask. Although we observed only a single β Cep pulsation mode from it, our analysis suggests that the pulsation originates from one of the similar components (Andersen et al. 1983) of the eclipsing binary.

TYC 8995-5052-1 = TIC 314139276. This has an eccentric orbit and few nearby sources that could contaminate the data. It is not clearly evident whether the signals originate from the early-B-type star.

V1388 Ori = TIC 337165095. This was discovered to be a β Cep pulsator in an eclipsing binary by Southworth & Bowman (2022b). These authors described it as a detached eclipsing binary with two early-B-type components that are significantly tidally distorted. They also reported two pulsation frequencies at 2.99 and 4.0 day^{-1}, which we confirm, together with some additional lower-frequency variability. If there was a β Cep pulsator in this system, it must be the more massive component, for which Southworth & Bowman (2022b) derived $M = 7.24 M_{\odot}$ and $R = 5.30 R_{\odot}$. This yields a pulsation constant $Q = 0.055$d, which is larger than the expected value for radial fundamental mode pulsation (see Stankov & Handler 2005 for a discussion). V1388 Ori could therefore be a pure g-mode pulsator.

V446 Cep = TIC 335265326. This was discovered to be an eclipsing binary with an orbital period of 3.81 days by Kazarovets et al. (1999), using Hipparcos satellite data, and reported as a β Cep pulsator by Southworth & Bowman (2022a). Although there is a long-period variable 20.″30 away, the magnitude difference, which is 6.210257 in the G band, suggests that the contaminator would have at best a minimal effect on the light curve of the target. We cannot completely rule out that the pulsation frequencies in the β Cep domain are combination frequencies of the g-mode signals.

V536 Mon = TIC 23548300. The binarity was first identified by Kukarkin et al. (1968) and corroborated by a number of authors, e.g., Kreiner (2004). It also has an eccentric orbit. The pulsations in both the β Cep and SPB frequency regimes are reported here for the first time. Given that the star is sufficiently below the β Cep instability strip in the theoretical H-R diagram, with a mass of about $5M_{\odot}$ (Figure 3), we are unsure whether the apparent β pulsations are not a result of rotational splitting of the SPB pulsations or combination frequencies. This star needs further investigation. We note in passing that there is a pulsating contaminating star, TIC 23548264 ($f = 7.281$ day^{-1}), which is not responsible for the strongest pulsations detected for V536 Mon.

V964 Sco = TIC 339567760. This belongs to the cluster NGC 6231 and has β Cep variability (Meingast et al. 2013). There are many possible contaminators from the cluster, such that it is not certain that both the eclipses and pulsations indeed come from the same star.

A.3. Likely Ellipsoidal Variables with β Cep Components

BD+48 658 = TIC 301263808. This star is an ellipsoidal variable. There is no contaminator within the aperture mask for a 5 mag difference. The nearby bright star BD+48 661 also does not cause notable contamination, hence the signals come from the target.

HD 13338 = TIC 347486043. This was identified as β Cep pulsator by Labadie-Bartz et al. (2020). Here, we report ostensible ellipsoidal variations in addition, but cannot confidently exclude a rotational origin. There is no significant contamination.

HD 232874 = TIC 266338052. The star could be an eclipsing or ellipsoidal variable with rotational modulation (Labadie-Bartz et al. 2020). These authors, however, also classified it as a β Cep pulsator. There could be some contamination from a nearby star (TYC 3718-137-1), 31.″29 away, which is about 3 mag fainter. The CROWDSAP parameters are 0.87358 and 0.92231 for Sectors 19 and 59, respectively. The optical companion may be a δ Scuti star.

HD 277132 = TIC 121064859. This appears to be an optical double. It is most likely an ellipsoidal, less likely a rotational variable with a β Cep pulsating component.

HD 300978 = TIC 458604640. This has a long-period variable, 2MASS J10414733-5644222 (4 mag dimmer), 114.″02 away from it. However, our analysis suggests that the signals come from the target.

HD 308106 = TIC 465870314. There is no significant contamination in the photometric aperture. This star is classified as an ellipsoidal or rotational variable or an eclipsing binary with a possible β Cep component.

HD 327010 = TIC 382486122. There is no significant contamination in the photometric aperture. The star is classified as an ellipsoidal variable with a possible β Cep component, although we cannot completely rule out a rotational origin for the 7.5537(6) days period.

HD 39716 = TIC 66975228. The star has no nearby contaminator. It is a possible ellipsoidal variable, with hybrid β Cep/SPB pulsations.

HD 55687 = TIC 178374964. There is a 1.1 mag brighter cool star (HD 55688) and two fainter hot stars all within 77″ of the target. Whereas the ellipsoidal variations should come from the target, these close-by objects could contribute to the short-period variations.

NGC 6913 82 = TIC 14621767. This belongs to an open cluster, NGC 6913 (Wang & Hu 2000). It is not clear whether the long-period variation we detected is due to ellipsoidal variability or rotation.

A.4. Rejected Objects

η Ori = TIC 4254645. This is a multiple system, comprising a detached eclipsing binary with an orbital period of 7.989 (3) days and one component showing g-mode pulsations and a noneclipsing binary with a period of 0.864 days and strong ellipsoidal variations (Mason et al. 2001; Southworth & Bowman 2022a). No β Cep pulsation was detected.

BD+61 675 = TIC 84342607. The eclipses that are present in the S19 30 minutes data can be attributed to the nearby eclipsing binary SZ Cam ($P = 2.7$ days). These eclipses are almost absent in the S59 2 minute data, but β Cep pulsations are still there with the same amplitude. We conclude that BD +61 675 is a noneclipsing β Cep star.

CD−59 4169 = TIC 383089500. The eclipses observed in this object's TESS light curve come from the target, but the pulsations come from the nearby TIC 383089586.

CPD−59 3141 = TIC 467066902. The eclipses are from a nearby source and the pulsation is too weak to be localized. Both the pulsational and eclipse signals are visible in Sector 64, a likely pointer to an external origin.

CW Cep = TIC 434893323. This was first discovered to be eclipsing by Alfonso-Garzón et al. (2012) and as a β Cep pulsator by Lee & Hong (2021). These authors obtained an orbital period of 2.72914(3) days and two dominant pulsation frequencies of 2.7265 and 5.3405 day^{-1}, which are close to being harmonically related, in agreement with what we also obtained from the QLP data. As both components are located in the β Cep domain, it is not clear which of the components is (or whether both are) pulsating. However, the pulsation constant $Q = P\sqrt{(\rho/rho_{\odot})}$, with the stellar mean density derived from the parameters listed by Lee & Hong (2021) for those two frequencies are 0.102/0.052 or 0.110/0.056 days, respectively. We therefore conclude that the pulsations in this system are due to gravity modes. Hence, this star is disqualified as a β Cep pulsator.

FZ CMa = TIC 125497512. FZ CMa was first discovered to be a double-lined spectroscopic binary by Neubauer (1943), eclipsing by Moffat & Vogt (1974), and β Cep by Southworth & Bowman (2022a). Detailed photometric and spectroscopic analyses of the system have been presented in the literature (e.g., Moffat et al. 1983; Southworth & Bowman 2022a). The pulsation spectrum is dominated by a 2.7 day^{-1} signal and possible harmonics and subharmonics. The masses that Southworth & Bowman (2022a) derive for this system are around 5 $M_{\odot}$. All this is evidence that FZ CMa is an SPB rather than a β Cep star.

HD 153772 = TIC 212415990. This was classified as β Cep pulsator by Pigulski & Pojmański (2008). However, it is located in a very crowded field, with nearby sources of relatively similar magnitude. It has very shallow eclipses as well. The light-curve shape of the single short-period variation (3.276 day^{-1}) resembles an ellipsoidal variation rather than a pulsation.

HD 154646 = TIC 380870688. The eclipses of the target are quite shallow and arise from the nearby Gaia source 5963347209003877888. The pulsation, however, appears to emanate from HD 154646.

HD 217919 = TIC 434723918. This was discovered to be a spectroscopic binary by Garmany (1972) and an eclipsing β Cep pulsator by Southworth & Bowman (2022a). We obtained an orbital period of 16.2080(9) days, which is in agreement with the period obtained by Southworth & Bowman (2022a), but in disagreement with that obtained by Garmany (1972). Southworth & Bowman (2022a) report significant third light and say the pulsations could arise in the third, noneclipsing, component. Again, the pulsation spectrum is consistent with a harmonic series of g-mode pulsations. We suspect that this system is a rapidly oscillating representative of the SPB stars.

HD 308111 = TIC 465869053. The light curve causing the longer-period variations appears to be of rotational instead of ellipsoidal origin.

LS II+23 34 = TIC 360661624. The eclipses come from the target, $P_{\rm orb}$ = 10.9815 days. The pulsations come from nearby LS II +23 36.

LS CMa = TIC 63427664. This was classified as a poor β Cep candidate in an eclipsing binary by Southworth & Bowman (2022a). As the single observed frequency not of orbital origin is below the β Cep regime, we reject this object from our candidate list.

V Pup = TIC 269562415. This was identified by Budding et al. (2021) as a massive close binary system of Algol-type evolution and a secondary that had experienced a mass ejection instead of a mass transfer. Contrary to these authors, we do not find any coherent periodic variability, apart from the eclipses. There seem to be instrumental effects and/or stochastic light variations present in the light curves of this bright object, but no β Cep pulsations.

ORCID iDs

Christian I. Eze https://orcid.org/0000-0003-3119-0399
Gerald Handler https://orcid.org/0000-0001-7756-1568

References

Aerts, C. 2021, RvMP, 93, 015001
Aerts, C., Christensen-Dalsgaard, J., & Kurtz, D. W. 2010, Asteroseismology (Dordrecht: Springer)
Aerts, C., & De Cat, P. 2003, SSRv, 105, 453
Aerts, C., Mathis, S., & Rogers, T. M. 2019, ARA&A, 57, 35
Alfonso-Garzón, J., Domingo, A., Mas-Hesse, J. M., & Giménez, A. 2012, A&A, 548, A79
Andersen, J., Clausen, J. V., Nordstroem, B., & Reipurth, B. 1983, A&A, 121, 271
Anderson, R. I., & Riess, A. G. 2018, ApJ, 861, 36
Avvakumova, E. A., Malkov, O. Y., & Kniazev, A. Y. 2013, AN, 334, 860
Balona, L. A. 2022, arXiv:2212.10776
Balona, L. A., & Ozuyar, D. 2020, MNRAS, 493, 5871
Balona, L. A., & Ozuyar, D. 2021, ApJ, 921, 5
Baran, A. S., & Koen, C. 2021, AcA, 71, 113
Batten, A. H. 2005, Ap&SS, 296, 3
Bowman, D. M. 2020, FrASS, 7, 70
Bowman, D. M., Aerts, C., Johnston, C., et al. 2019a, A&A, 621, A135
Bowman, D. M., Burssens, S., Pedersen, M. G., et al. 2019b, NatAs, 3, 760
Bowman, D. M., Burssens, S., Simón-Díaz, S., et al. 2020, A&A, 640, A36
Bowman, D. M., Vandenbussche, B., Sana, H., et al. 2022, A&A, 658, A96
Brancewicz, H. K., & Dworak, T. Z. 1980, AcA, 30, 501
Brasseur, C. E., Phillip, C., Fleming, S. W., Mullally, S. E., & White, R. L. 2019, Astrocut: Tools for creating cutouts of TESS images, Astrophysics Source Code Library, ascl:1905.007
Bruntt, H., & Southworth, J. 2008, JPhCS, 118, 012012
Budding, E., Love, T., Blackford, M. G., Banks, T., & Rhodes, M. J. 2021, MNRAS, 502, 6032
Burke, C. J., Levine, A., Fausnaugh, M., et al. 2020, TESS-Point: High precision TESS pointing tool, Astrophysics Source Code Library, ascl:2003.001
Burssens, S., Bowman, D. M., Michielsen, M., et al. 2023, NatAs, 7, 913
Burssens, S., Simón-Díaz, S., Bowman, D. M., et al. 2020, A&A, 639, A81
Chen, X., Ding, X., Cheng, L., et al. 2022, ApJS, 263, 34
Cousins, A. W. J., Lagerweij, H. C., & Shillington, F. A. 1969, MNSSA, 28, 63
De Mey, K., Aerts, C., Waelkens, C., et al. 1997, A&A, 324, 1096
Drobek, D., Pigulski, A., Shobbrook, R., & Narwid, A. 2010, AN, 331, 1077
Dvorak, S. W. 2004, IBVS, 5542, 1
Eggleton, P. P., & Tokovinin, A. A. 2008, MNRAS, 389, 869
Feast, M. W., Stoy, R. H., Thackeray, A. D., & Wesselink, A. J. 1961, MNRAS, 122, 239
Feinstein, A. D., Montet, B. T., Foreman-Mackey, D., et al. 2019, PASP, 131, 094502
Flower, P. J. 1996, ApJ, 469, 355
Freyhammer, L. M., Hensberge, H., Sterken, C., et al. 2005, A&A, 429, 631
Gaia Collaboration, Prusti, T., de Bruijne, J. H. J., et al. 2016, A&A, 595, A1
Gaia Collaboration, Vallenari, A., Brown, A. G. A., et al. 2023, A&A, 674, A1
Gaposchkin, S. 1943, PASP, 55, 192
Garmany, C. D. 1972, AJ, 77, 38
Gough, D. 1985, SoPh, 100, 65
Handler, G. 2013, in Planets, Stars and Stellar Systems, ed. T. D. Oswalt & M. A. Barstow, Vol. 4 (Dordrecht: Springer), 207
Handler, G., Pigulski, A., Daszyńska-Daszkiewicz, J., et al. 2019, ApJL, 873, L4
Handler, G., Rybicka, M., Popowicz, A., et al. 2017, MNRAS, 464, 2249
Handler, G., & Schwarzenberg-Czerny, A. 2013, A&A, 557, A1
Herrero, A., Kudritzki, R. P., Vilchez, J. M., et al. 1992, A&A, 261, 209
Higgins, M. E., & Bell, K. J. 2023, AJ, 165, 141
Huang, C. X., Vanderburg, A., Pál, A., et al. 2020a, RNAAS, 4, 204
Huang, C. X., Vanderburg, A., Pál, A., et al. 2020b, RNAAS, 4, 206
IJspeert, L. W., Tkachenko, A., Johnston, C., et al. 2021, A&A, 652, A120
Jaschek, M., & Egret, D. 1982, in IAU Symp. 98, Be Stars, ed. M. Jaschek & H. G. Groth (Dordrecht: D. Reidel), 261
Jerzykiewicz, M. 1980, Nonradial and Nonlinear Stellar Pulsation (Berlin: Springer), 125
Jerzykiewicz, M., & Sterken, C. 1977, AcA, 27, 365
Kallrath, J., & Milone, F. E. 2009, Eclipsing Binary Stars: Modeling and Analysis (New York: Springer-Verlag)
Kazarovets, E. V., Samus, N. N., Durlevich, O. V., et al. 1999, IBVS, 4659, 1
Kirk, B., Conroy, K., Prša, A., et al. 2016, AJ, 151, 68
Kobulnicky, H. A., Kiminki, D. C., Lundquist, M. J., et al. 2014, ApJS, 213, 34
Kovács, G., Zucker, S., & Mazeh, T. 2002, A&A, 391, 369
Kreiner, J. M. 2004, AcA, 54, 207
Kukarkin, B. V., Efremov, Y. N., Frolov, M. S., et al. 1968, IBVS, 311, 1
Kurtz, D. W., Shibahashi, H., Murphy, S. J., Bedding, T. R., & Bowman, D. M. 2015, MNRAS, 450, 3015
Labadie-Bartz, J., Handler, G., Pepper, J., et al. 2020, AJ, 160, 32
Lee, J. W., & Hong, K. 2021, AJ, 161, 32
Lee, O. J. 1910, ApJ, 32, 300
Lehmann, H., Harmanec, P., Aerts, C., et al. 2001, A&A, 367, 236
Lenz, P., & Breger, M. 2005, CoAst, 146, 53
Mason, B. D., Wycoff, G. L., Hartkopf, W. I., Douglass, G. G., & Worley, C. E. 2001, AJ, 122, 3466
Meingast, S., Handler, G., & Shobbrook, R. R. 2013, A&A, 559, A108
Moffat, A. F. J., & Vogt, N. 1974, A&A, 30, 381
Moffat, A. F. J., & Vogt, N. 1975, A&AS, 20, 125
Moffat, A. F. J., Vogt, N., Vaz, L. P. R., & Gronbech, B. 1983, A&A, 120, 278
Neilson, H. R., & Ignace, R. 2015, A&A, 584, A58
Neubauer, F. J. 1943, ApJ, 97, 300
Otero, S. A. 2003, IBVS, 5480, 1
Otero, S. A., & Wils, P. 2005, IBVS, 5644, 1

Pamyatnykh, A. A. 1999, AcA, 49, 119
Pamyatnykh, A. A., Dziembowski, W. A., Handler, G., & Pikall, H. 1998, A&A, 333, 141
Pedersen, M. G., Chowdhury, S., Johnston, C., et al. 2019, ApJL, 872, L9
Percy, J. R., & Au-Yong, K. 2000, IBVS, 4825, 1
Pigulski, A., & Pojmański, G. 2008, A&A, 477, 917
Prša, A., Conroy, K. E., Horvat, M., et al. 2016, ApJS, 227, 29
Ricker, G. R., Winn, J. N., Vanderspek, R., et al. 2015, JATIS, 1, 014003
Russell, H. N. 1948, HarMo, 7, 181
Sana, H., de Mink, S. E., de Koter, A., et al. 2012, Sci, 337, 444
Sana, H., Le Bouquin, J. B., Lacour, S., et al. 2014, ApJS, 215, 15
Scargle, J. D. 1982, ApJ, 263, 835
Shi, X.-d., Qian, S.-b., Zhu, L.-y., et al. 2024, ApJS, 271, 28
Shibahashi, H., & Aerts, C. 2000, ApJL, 531, L143
Southworth, J. 2012, Orbital Couples: Pas de Deux in the Solar System and the Milky Way, ed. F. Arenou & D. Hestroffer, 51
Southworth, J. 2015, EPJWC, 101, 04001
Southworth, J., & Bowman, D. M. 2022a, MNRAS, 513, 3191
Southworth, J., & Bowman, D. M. 2022b, Obs, 142, 161
Southworth, J., Bowman, D. M., & Pavlovski, K. 2021, MNRAS, 501, L65
Southworth, J., Bowman, D. M., Tkachenko, A., & Pavlovski, K. 2020, MNRAS, 497, L19
Stankov, A., & Handler, G. 2005, ApJS, 158, 193
Steindl, T., Zwintz, K., Barnes, T. G., Müllner, M., & Vorobyov, E. I. 2021, A&A, 654, A36
Sterken, C., Duerbeck, H. W., Hensberge, H., et al. 1985, A&AS, 60, 1
Sterken, C., & Jerzykiewicz, M. 1993, SSRv, 62, 95
Straizys, V., Meistas, E., Vansevicius, V., & Goldberg, E. P. 1989, VilOB, 83, 3
Thackeray, A. D., Tritton, S. B., & Walker, E. N. 1973, MmRAS, 77, 199
Thoul, A., Aerts, C., Dupret, M. A., et al. 2003, A&A, 406, 287
Tkachenko, A., Pavlovski, K., Johnston, C., et al. 2020, A&A, 637, A60
Torres, G., Andersen, J., & Giménez, A. 2010, A&ARv, 18, 67
Wachmann, A. A. 1973, A&A, 25, 157
Waelkens, C. 1991, A&A, 246, 453
Waelkens, C., Aerts, C., Kestens, E., Grenon, M., & Eyer, L. 1998, A&A, 330, 215
Walker, M. F. 1951, PASP, 63, 35
Wang, J. J., & Hu, J. Y. 2000, A&A, 356, 118
Zari, E., Rix, H. W., Frankel, N., et al. 2021, A&A, 650, A112